"Notes of Fluid Mechanics"

Piero Olla

ISAC-CNR and INFN, Sez. Cagliari, I–09042 Monserrato, Italy

June 9, 2022

Contents

1 Continuous limit

We are interested in the description of fluids at macroscopic scales such that effects from the discrete nature of the medium can be disregarded. In other words, we are focusing on phenomena at scales l, much larger than the typical molecular separation a_0. The typical number N_l of molecules in a volume V_l of linear size l, therefore, will be very large,

$$N_l \sim (l/a_0)^3 \gg 1, \tag{1.1}$$

and the relative fluctuation $\delta N_l/N_l$ very small; we can thus approximate instantaneous quantities with their average with respect to fluctuations from discrete effects, $N_l \simeq \langle N_l \rangle$.

The lenght l defines the spatial scale of variation of the macroscopic variables of interest in the fluid. This allows us to define macroscopic quantities through a process of of coarse graining at an intermediate scale a, $a_0 \ll a \ll l$, such that the variation of macroscopic quantities at scale a is small, and the relative fluctuation magnitude of these quantities is small as well.

Let us start with the density n. We first define a corse-grained density

$$n_a(\mathbf{x},t) = \frac{N_a(\mathbf{x},t)}{V_a} \simeq \frac{\langle N_a(\mathbf{x},t)\rangle}{V_a} = \langle n_a(\mathbf{x},t)\rangle \tag{1.2}$$

and then exploit the condition $a_0 \ll a \ll l$ to formally carry out the continuous limit

$$n(\mathbf{x},t) = \lim_{a\to 0} n_a(\mathbf{x},t). \tag{1.3}$$

We follow the same procedure with the current density $\mathbf{J}$ and fluid velocity $\mathbf{u}(\mathbf{x},t)$. We indicate with $\mathbf{v}_i(t)$ the instantaneous velocities of the molecules in $V_a = V_a(\mathbf{x})$ and define

$$n(\mathbf{x},t)\mathbf{u}(\mathbf{x},t) = \mathbf{J}(\mathbf{x},t) = \lim_{a\to 0} V_a^{-1} \sum_{i\in V_a} \mathbf{v}_i(t), \tag{1.4}$$

We shall focus in this course on systems composed of a single species of molecules. The density n and the current density $\mathbf{J}$ will then be proportional, through the molecular mass m, to the mass density ρ and the mass current density J_m:

$$\rho = mn, \qquad \mathbf{J}_m = m\mathbf{J}. \tag{1.5}$$

Macroscopic quantities such as the density n and the fluid velocity $\mathbf{u}$ are sums of microscopic contributions by the individual molecules. If the interaction of the molecules is not too strong, it is possible to consider the microscopic contributions as statistical independent. This hypthesis allows us to estimate the fluctuation amplitude of macroscopic quantities. Suppose we have N molecules contributing to the sum; indicate with x_i the contribution by the i_th molecule and with $X = \sum_i^N x_i$ the macroscopic quantity. We suppose the x_i to be identically distributed variables with average $\langle x_i\rangle = \mu_x$ and RMS $\langle (x_i-\mu)^2\rangle^{1/2} = \sigma_x$. We have for the average of X:

$$\mu_X = N\mu_x \tag{1.6}$$

and for its RMS:

$$\sigma_X^2 = \langle (X-\mu_X)^2\rangle = \sum_{ij} \langle (x_i-\mu)(x_j-\mu)\rangle. \tag{1.7}$$

Statistical independence, however, implies that the x_i's are uncorrelated:

$$\langle (x_i-\mu)(x_j-\mu)\rangle = \sigma^2\delta_{ij}. \tag{1.8}$$

Hence only terms with $i=j$ in Eq. (1.7) contribute to σ_X^2 and we are left with

$$\sigma_X^2 = N\sigma_x^2. \tag{1.9}$$

Thus, for large N,

$$\frac{\delta X}{X} \sim \frac{\sigma_X}{\mu_X} \sim N^{-1/2}. \tag{1.10}$$

As an application, let us evaluate the fluctuation in the occupation number N_a in a volume V_a. Indicate with N the number of molecules in the fluid that could potentially lie in V_a and introduce a random variable x_i that is $= 1$ if $i \in V_a$, $= 0$ otherwise. We consider identically distributed molecules, indicating with p the probability that a given molecule lies in V_a at a given time. We immediately find

$$\mu_x = p \quad \text{and,} \qquad \sigma_x^2 = \langle x_i^2 \rangle - \mu_x^2 = p - p^2, \tag{1.11}$$

and therefore, from Eqs. (1.6) and (1.9),

$$\mu_{N_a} = pN, \quad \sigma_{N_a}^2 = (p - p^2)N, \tag{1.12}$$

which implies

$$\frac{\delta N}{N} \sim \frac{\sqrt{(p - p^2)N}}{pN} = (1 - p)^{1/2} N^{-1/2} \sim N^{-1/2}. \tag{1.13}$$

We can carry out the same reasoning with the other macroscopic quantities we have introduced in this section, and we obtain

$$\frac{\delta n_a}{n} \sim \frac{\delta J_a}{J} \sim \frac{\delta u_a}{u} \sim \frac{\delta N_a}{N_a} \sim (na^3)^{-1/2}. \tag{1.14}$$

The condition for a continuous limit can then be reformulated as

$$nl^3 \gg 1. \tag{1.15}$$

We conclude the section by introducing a concept that will accompany us throughout the course: that of fluid element (or fluid parcel). A "fluid element" is simply a portion of the fluid that, on time scales of interest, is not significantly deformed by the gradients of $\mathbf{u}(\mathbf{x}, t)$. We define more precisely fluid element by the condition that points on its surface move with the local fluid velocity $\mathbf{u}(\mathbf{x}, t)$. This requirement guarantees that the mass in the volume remains constant, even though molecules continuously cross the volume boundary. We use the notation V_L to make clear that a given volume (non necessarily a fluid element) is transported by the flow. Note that the motion of a fluid element is identical to that of a solid particle small enough to be transported by the fluid without exerting any feedback force. We call such an object a passive tracer.

1.1 Suggested reading

- L.D. Landau and E.M. Lifshitz, "Statistical Physics" Vol. 5, Secs. 1, 2 and 114 (Pergamon Press, 1980)

2 Fluid kinematics

2.1 Lagrangian and Eulerian description of a flow

We can achieve a kinematic description of a flow basically in two ways:

- We can work in a "laboratory frame" and study the evolution of the flow at a fixed position in space, which is called an Eulerian approach.
- We can study the evolution of the flow measured by a fluid parcel transported by that flow field, which is called a Lagrangian approach.

An Eulerian description may, in some respect, look more natural; indeed, most evolution equations, such as the Navier-Stokes equation, are written in an Eulerian frame; likewise, most experimental measurements, e.g., that of $\mathbf{u}(\mathbf{x}, t)$ by an anemometer, are carried out at a fixed position of space. However, there are counterexamples: the Bernoulli law is an example of an evolution equation in a Lagrangian frame; experiments in wind tunnels are often based on seeding the flow with tracer particles, and in one way or another, bring into play ideas from a Lagrangian point of view.

The first step in the Lagrangian description of a flow, is to define the coordinate of a fluid parcel. Indicate with

$$\mathbf{x}_L(t) \equiv \mathbf{x}_L(t|\mathbf{x}_0, t_0), \tag{2.1}$$

the position at time t of the fluid element that at time t_0 was (or will be) at $\mathbf{x}_0$. We call $\mathbf{x}_L(t)$ a Lagrangian coordinate and its trajectory a Lagrangian trajectory.

The couple $(\mathbf{x}_0, t_0)$ plays the role of a label identifying the parcel and is arbitrary: the time t_0 is itself arbitrary (in the case of a solid, it would be natural to choose $\mathbf{x}_0$ as the coordinate of the undeformed body, in such a way that $x_L(t|\mathbf{x}_0, t_0) - \mathbf{x}_0$ is the deformation; t_0 is then defined in consequence); in general we could identify the parcel with a label that does not bear any reference to points the parcel visits in its motion. The choice in Eq. (2.1), however, allows us to identify

$$\mathbf{x}_L(t|\mathbf{x}_0, t) = \mathbf{x}_0, \tag{2.2}$$

which will come handy when switching from a Lagrangian to an Eulerian description.

From $\mathbf{x}_L$ we define the Lagrangian velocity of the parcel:

$$\mathbf{u}_L(t) \equiv \mathbf{u}_L(t|\mathbf{x}_0, t_0) = \dot{\mathbf{x}}_L(t|\mathbf{x}_0, t_0) \equiv \partial_t \mathbf{x}_L(t|\mathbf{x}_0, t_0). \tag{2.3}$$

We can express the Lagrangian velocity $\mathbf{u}_L(t)$ in term of the Eulerian velocity $\mathbf{u}(\mathbf{x}, t)$:

$$\mathbf{u}_L(t|\mathbf{x}_0, t_0) = \mathbf{u}(\mathbf{x}_L(t|\mathbf{x}_0, t_0), t) \Rightarrow \mathbf{u}_L(t|\mathbf{x}_0, t) = \mathbf{u}(\mathbf{x}_0, t). \tag{2.4}$$

By combining Eqs. (2.3) and (2.4) we obtain the equation of motion of a fluid parcel in an Eulerian flow field $\mathbf{u}(\mathbf{x}, t)$

$$\dot{\mathbf{x}}_L(t) = \mathbf{u}(\mathbf{x}_L(t), t). \tag{2.5}$$

The concept of Lagrangian trajectory is closely related to that of streamline (or flow line) The streamlines of a vector field $\mathbf{U}(\mathbf{x})$ are defined as the trajectories of the points obeying the equation

$$\dot{\mathbf{x}}_s(t) = \mathbf{U}(\mathbf{x}_s(t)); \tag{2.6}$$

indeed, the vector $\mathbf{U}(\mathbf{x})$ is by construction tangent at $\mathbf{x}$ of the particular streamline passing through the point (which tells that if $\mathbf{U}(\mathbf{x}) \neq 0$, there is only one field line crossing $\mathbf{x}$). We thus see that the Lagrangian trajectories of a time-independent flow $\mathbf{u} = \mathbf{u}(\mathbf{x})$, are the streamlines of the flow. We can easily convince ourselves that they also coincide with the so-called streak lines, which is the set of points obtained by superposing all Lagrangian trajectories $\mathbf{x}_L(t|\mathbf{x}_0, t_0)$ originating in $\mathbf{x}_0$ for different values of t_0 (think of it as the result of the continuous injection at x_0, of tracers which are then transported away by the flow). From Eq. (2.5) we can derive the equation for the instantaneous streamlines of a time-dependent flow field at a given time t:

$$\dot{\mathbf{x}}_s(s) = \mathbf{u}(\mathbf{x}_s(s), t). \tag{2.7}$$

We see that in this case, the instantaneous flow lines, the Lagrangian trajectories and the streak lines of the field do not coincide.

We can extend the definitions in Eqs. (2.1) and (2.3) to the case of a generic field $\phi(\mathbf{x}, t)$. We indicate with

$$\phi_L(t|\mathbf{x}_0, t_0) = \phi(\mathbf{x}_L(t|\mathbf{x}_0, t_0), t) \tag{2.8}$$

the value of the field measured along the path of a fluid parcel. This expression allows us to characterize the dependence of the Lagrangian field on the variable t. Let us analyze the dependence on the initial position $\mathbf{x}_0$. The change of variable $\phi(\mathbf{x}_L(t|\mathbf{x}_0), t) = \phi_L(t|\mathbf{x}_0)$ is an example of what in mathematical jargon is called the pull-back $\phi_L = \mathbf{x}_L^*\phi$ of ϕ by $\mathbf{x}_L$: the value of the field ϕ is *pulled back* from the the point $\mathbf{x}_L$ to its original position $\mathbf{x}_0$ at time t_0. We can this look at ϕ_L both as the value of ϕ measured by the fluid parcel along the trajectory $\mathbf{x}_L$, and as the value of ϕ that the flow transports from $\mathbf{x}_0$ to the current position. In both cases, the dependence of ϕ_L on t has a component that is not associated with transport, which corresponds to the explicit time dependence of $\phi(\mathbf{x}_L, t)$. An example of field $\phi = \phi(\mathbf{x})$ independent of time is that of a fixed orography; $\mathbf{u}(\mathbf{x}, t)$ could be, say, a horizontal wind velocity field. If ϕ_L is constant, we say that the field ϕ is "frozen in the flow"; we call this process Lagrangian transport; an example is the transport of a dye in an incompressible flow: in the absence of diffusion, the dye concentration at the current position $\mathbf{x}_L$ is equal to the concentration at the initial point $\mathbf{x}_0$.

At this point, we may want to be able to switch from an Eulerian to a Lagrangian description of the flow. The operation is carried out by means of the so-called material derivative

$$D_t = \partial_t + \mathbf{u}(\mathbf{x}, t) \cdot \nabla. \tag{2.9}$$

We verify in fact that

$$\begin{aligned}\partial_t \phi_L(t|\mathbf{x}_0,t_0)|_{t_0=t} &= [\partial_t + \mathbf{u}_L(t|\mathbf{x}_0,t_0)\cdot\nabla_{\mathbf{x}_L}]\phi(\mathbf{x}_L(t|\mathbf{x}_0,t_0),t)|_{t_0=t} \\ &= [\partial_t + \mathbf{u}(\mathbf{x}_0,t)\cdot\nabla_{\mathbf{x}_0}]\phi(\mathbf{x}_0,t).\end{aligned}$$

More concisely

$$\partial_t \phi_L(t|\mathbf{x},t_0)|_{t_0=t} = D_t\phi(\mathbf{x},t). \tag{2.10}$$

The term $\mathbf{u}\cdot\nabla$ in Eq. (2.9) is called advection, which is the contribution to the variation of ϕ_L from the motion of the fluid parcel along the Lagrangian trajectory $\mathbf{x}_L$. Note that $\mathbf{t}_0$ is arbitrary, and can therefore be chosen in such a way that Eq. (2.10) is satisfied. In the case ϕ is frozen in the flow, $\dot{\phi}_L = 0 \Rightarrow D_t\phi = 0$, which implies

$$\partial_t\phi(\mathbf{x},t) = -\mathbf{u}(\mathbf{x},t)\cdot\nabla\phi(\mathbf{x},t). \tag{2.11}$$

The material derivative describes the evolution of a field in the reference frame of the moving fluid element. By construction, it is therefore unaffected by the Galilean shift $(\mathbf{x},t) \to (\mathbf{x}',t) = (\mathbf{x}-\mathbf{U}t,t)$:

$$(\partial_t + (\mathbf{u}+\mathbf{U})\cdot\nabla)\phi(\mathbf{x}-\mathbf{U}t,t) = (\partial_t + \mathbf{u}\cdot\nabla)\phi(\mathbf{x}',t). \tag{2.12}$$

2.2 Lagrangian transport of a vector field

In the following, we will have to deal a lot with transport of vector quantities, such as the fluid velocity and the vorticity; dealing with electrically conducting fluids, we may need to include the electric density current and the magnetic field in the description.

The Lagrangian transport of a vector field presents several subtleties. We discuss them one by one.

The simple way to extend the idea of Lagrangian transport from a scalar to a vector field $\mathbf{v}(\mathbf{x},t)$ is to require that the $\mathbf{v}_L(t|\mathbf{x}_0,t_0) = \mathbf{v}(\mathbf{x}_L(t|\mathbf{x}_0,t_0)$ along the fluid trajectories defined by $\dot{\mathbf{x}}_L(t) = \mathbf{u}(\mathbf{x}_L,t)$. While the stem of vecctor $\mathbf{v}_L$ is dragged along the trajectory $\mathbf{x}_L$, neither the magnitude nor the direction of the vector will change; the operation is usually called parallel transport. Parallel transport is trivial in Euclidean space, as we can utilize global Cartesian coordinates which translate the condition $\dot{\mathbf{v}}_L = 0$ into identical conditions on the components: $\dot{v}_{Li} = 0$. However, there are situations of practical interest in which the fluid flow develops in a curved space. Examples could be the fluid flow on a cell surface or the wind dynamics at scales such that the earth's curvature cannot be disregarded.

For example, consider the transport of a vector on the earth surface. Take a vector $\mathbf{v}$ in Rome directed north, and displace it parallel to itself to Chicago, which lies roughly at the same latitude as Rome, but at the longitude $\phi \simeq \pi/2$ west.

Indicate with $\mathbf{v}_p$ the new vector. From space, the two vectors look identical, but while in Rome $\mathbf{v}$ points north, in Chicago it points north-west: the component of $\mathbf{v}$ on the equatorial plane, which in Rome is perpendicular to the earth parallel in Chicago is tangent to it; direction of the meridian line, however, has changed; this simple observation informs us that to describe in coordinate the transport of a vector at distance such as the one from Rome to Chicago, we need to work with global coordinates that are necessarily curvilinear.

We see from Eq. (2.10) that the term that causes trouble in expressing the condition $\dot{\mathbf{v}}_L = 0$ in coordinates, is the advection $\mathbf{u} \cdot \mathbf{v}$. The trouble comes from the dependence of the basis vectors $\mathbf{e}_i$ on the coordinate; we need to be careful in this case to distinguish covariant indices (those of the basis) and contravariant indices (those of the components); we thus adopt the summation convention and write

$$\mathbf{v} = v^i \mathbf{e}_i, \qquad \nabla = \mathbf{e}^i \partial_i, \qquad \mathbf{e}_i \cdot \mathbf{e}^j = \delta_{ij}, \tag{2.13}$$

where we have introduced the contravariant basis $\mathbf{e}^i$ to guarantee that the differential of a scalar remains a scalar:

$$\mathrm{d}\mathbf{x} \cdot \nabla f = \mathrm{d}x^i \partial_i f \equiv \mathrm{d}f. \tag{2.14}$$

We can now evaluate the components of the advection term:

$$(\mathbf{u} \cdot \mathbf{v})^i = [u^k \partial_k \mathbf{e}_j v^j]^i = u^k \partial_k v^j + u^k v^j (\partial_k \mathbf{e}_j)^i = u^k [\delta^i_j \partial_k + \Gamma^i_{jk}] v^j, \tag{2.15}$$

where

$$\Gamma^i_{kj} = (\partial_k \mathbf{e}_j)^i \equiv \mathbf{e}^i \cdot (\partial_k \mathbf{e}_j) \tag{2.16}$$

is called the Christoffel symbol and the tensor $[\delta^i_j \partial_k + \Gamma^i_{kj}] v^j$ is called the covariant derivative.

We shall confine our analysis in the rest of these notes to phenomena taking place at such a scale that effects from a possible curvature of the embedding space can be disregarded; we will then assume Cartesioan throughout, without distinguishing covariant from controvariant indices.

Now that we have been able to clarify the meaning of advection of a vector as an operation of parallel transport, we may ask whether parallel transport and Lagrangian transport are the same things. The fact is that we may intepret a vector field as a derived object, namely the set of vectors tangent to a streamlines' field; the differential $\mathbf{v}\mathrm{d}s$ would represent then an infinitesimal segment of a streamline, and the question arises whether Lagrangian transport should refer to the vector $\mathbf{v}$ or streamlines. The situation is illustrated in Fig. 1: in the case of parallel transport, one shifts the vector parallel to itself by shifting its stem; in the case streamlines are being transported, one ought to simultaneously shift both stem and tip of the vector $\mathbf{v}\mathrm{d}s$, which are two points of a streamline. We shall speak of Lagrangian transport of a vector field $\mathbf{v}$ and refer to $\mathbf{v}$ as a frozen vector field, when the points on the streamlines of $\mathbf{v}$ are transported by the flow like passive tracers.

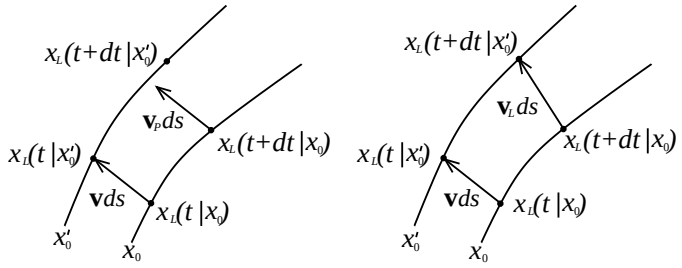

Figure 1: Comparison of parallel transport (left) and Lagrangian transport (right) of a vector field $\mathbf{v}$ by the flow $\mathbf{u}$.

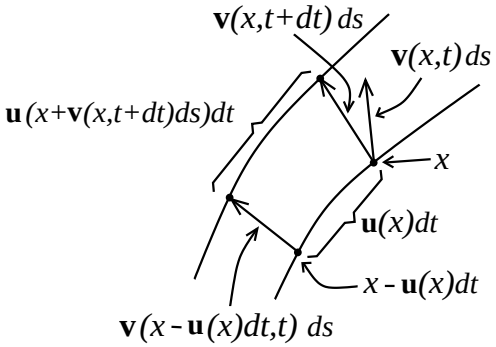

Figure 2: Graphical derivation of the evolution equation for a frozen vector field $\mathbf{v}$. The curved lines are the streamlines of $\mathbf{u}$.

An example of a vector field transported parallel to itself is the fluid velocity if both viscous and pressure forces are negligible (Burgers dynamics). Examples of vector fields frozen in the flow are the vorticity in a zero viscosity fluid and the magnetic field in a zero viscosity - zero resistivity fluid.

Let us derive the evolution equation for a frozen vector field. The operation is illustrated in Fig. 2. We want to calculate the difference $\mathbf{v}(x, t+\mathrm{d}t) - \mathbf{v}(\mathbf{x}, t)$ in the case $\mathbf{v}$ is frozen in $\mathbf{u}$. The shift of tip and stem of vector $\mathbf{v}$ along the field lines of $\mathbf{u}$ is carried out considering a snapshot $\mathbf{u}(\mathbf{x}) \equiv \mathbf{u}(\mathbf{x}, t)$ at fixed t (the dependence of $\mathbf{u}(\mathbf{x}, t)$ on t produces higher order differentials that are disregarded). We see that $\mathbf{v}(\mathbf{x}, t+\mathrm{d}t)$ is the vector sum

$$\begin{aligned} &\mathbf{v}(\mathbf{x} - \mathbf{u}(\mathbf{x})\mathrm{d}t, t)\mathrm{d}s + \mathbf{u}(\mathbf{x} + \mathbf{v}(\mathbf{x}, t+\mathrm{d}t)\mathrm{d}s)\mathrm{d}t - \mathbf{u}(\mathbf{x}, t) \\ &\simeq \mathbf{v}(\mathbf{x}, t)\mathrm{d}s - \mathbf{u}(\mathbf{x}, t)\cdot\nabla\mathbf{v}(\mathbf{x}, t)\mathrm{d}s\mathrm{d}t + \mathbf{v}(\mathbf{x}, t)\cdot\nabla\mathbf{u}(\mathbf{x})\mathrm{d}s\mathrm{d}t \end{aligned}$$

We thus obain for the time derivative of a vector field frozen in $\mathbf{u}$:

$$\partial_t\mathbf{v}(\mathbf{x}, t) = -\mathbf{u}(\mathbf{x}, t)\cdot\nabla\mathbf{v}(\mathbf{x}, t) + \mathbf{v}(\mathbf{x}, t)\cdot\nabla\mathbf{u}(\mathbf{x}, t) := -\mathcal{L}_u\mathbf{v}(\mathbf{x}, t). \tag{2.17}$$

The operator $\mathcal{L}_\mathbf{u}\mathbf{v} = \mathbf{u}\cdot\nabla\mathbf{v} - \mathbf{v}\cdot\nabla\mathbf{u}$ is called the Lie derivative of $\mathbf{v}$ in the direction of $\mathbf{u}$.

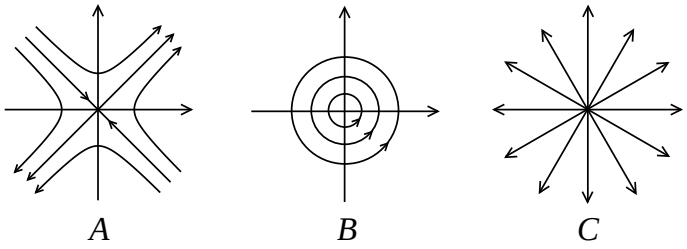

Figure 3: Sketch of 2D flows that are locally pure strain (A), pure vortical (B) or pure compressional (C).

2.3 Vorticity, rate of strain and compression rate

The dynamics of fluids is governed by the stresses generated by the relative motions within the fluid. In the case of a simple fluid, these stresses are generated locally by the gradient of the fluid velocity. Locality of the dynamics allows us to use Cartesian coordinates (provided we stick to a local description of the flow) when the flow evolves on a curved surface.

Let us decompose the tensor $\nabla\mathbf{u}$ into its trace component and its symmetric zero-trace and antisymmetric components:

$$\partial_i u_j = \frac{\delta_{ij}}{3}\nabla\cdot\mathbf{u} + \frac{1}{2}\Big(\partial_i u_j + \partial_j u_i - \frac{2\delta_{ij}}{3}\nabla\cdot\mathbf{u}\Big) + \frac{1}{2}\Big(\partial_i u_j - \partial_j u_i\Big). \tag{2.18}$$

We can express the antisymmetric component $(1/2)[\nabla\mathbf{u} - (\nabla\mathbf{u})^t]$ in terms of the vorticity

$$\boldsymbol{\omega} = \nabla\times\mathbf{u}, \tag{2.19}$$

$$\nabla\mathbf{u} - (\nabla\mathbf{u})^t = \begin{pmatrix} 0 & \omega_3 & -\omega_2 \\ -\omega_3 & 0 & \omega_1 \\ \omega_2 & -\omega_1 & 0 \end{pmatrix}. \tag{2.20}$$

The symmetric zero-trace component of $\nabla\mathbf{u}$

$$\dot{s}_{ij} = \partial_i u_j + \partial_j u_i - \frac{2\delta_{ij}}{3}\nabla\cdot\mathbf{u} \tag{2.21}$$

is called the rate of strain, and the remaining trace component $\nabla\cdot\mathbf{u}\delta_{ij}$ (taken with minus sign) is called the compression rate.

We show in Fig. 3 the streamlines of two-dimensional (2D) velocity fields which are locally purely vortical, purely compressional, or purely strain flow. Case A in Fig. 3 corresponds to a flow field $u_1 = sx_2$, $u_2 = sx_1$. We can obtain the streamlines for this flow field from Eq. (2.6), $\dot{x}_1 = sx_2$, $\dot{x}_2 = sx_1$, which implies $2\mathrm{d}x_1^2/\mathrm{d}t = sx_1x_2$, $2\mathrm{d}x_2^2/\mathrm{d}t = sx_2x_1$ and therefore $x_1^2 - x_2^2 = const.$, which is the equation for the

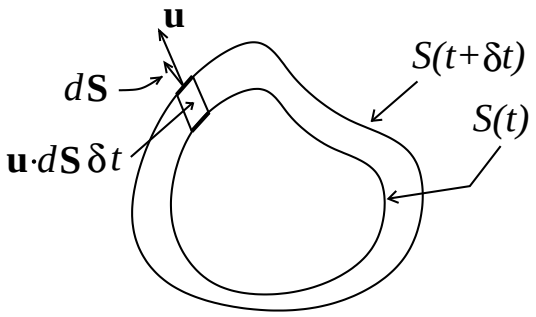

Figure 4: The motion of the boundary of a fluid volume, induced by the flow $\mathbf{u}$.

hyperboles shown in case A of Fig. 3. The same procedure in case B of Fig. 3 yields $x_1^2 + x_2^2 = const.$, which corresponds to the circular orbits in the figure (note that the flow field describes a fluid that rotates rigidly with angular frequency ω; such a flow is often called rotational, leaving the term vortical to situations in which ω varies with the distance from the origin).

The compression rate gives the volume change of a portion of the fluid induced by the flow $\mathbf{u}$; we illustrate the situation in Fig. 4. Indicate with $\mathrm{d}\mathbf{A}$ the oriented element of surface of the volume of fluid V. In the time interval δt the volume V changes by the amount

$$V(t+\delta t) - V(t) \simeq \delta t \int_{A(t)} \mathrm{d}\mathbf{A} \cdot \mathbf{u}(\mathbf{x}, t) = \delta t \int_{V(t)} \mathrm{d}V \, \nabla \cdot \mathbf{u}(\mathbf{x}, t). \tag{2.22}$$

The compression rate of a fluid element is therefore precisely

$$-\dot{V}/V = -\nabla \cdot \mathbf{u}. \tag{2.23}$$

A flow for which $\nabla \cdot \mathbf{u} = 0$ is called incompressible.

2.4 Application to Hamiltonian dynamics

We can utilize the techniques developed in the present section to characterize Hamiltonian flows. This is the flow of phase points in the 2N-dimensional phase space labeled by coordinates (p_i, q_i), $i = 1, \ldots N$, where N is the number of degrees of freedom of the system. In the case of a system with just one degree of freedom, the phase points are identified by the 2D vector

$$\mathbf{x} = \begin{pmatrix} p \\ q \end{pmatrix} \tag{2.24}$$

Hamilton's equations define the fluid velocity

$$\mathbf{u} = \dot{\mathbf{x}} = \begin{pmatrix} -\partial_q H \\ \partial_p H \end{pmatrix}, \tag{2.25}$$

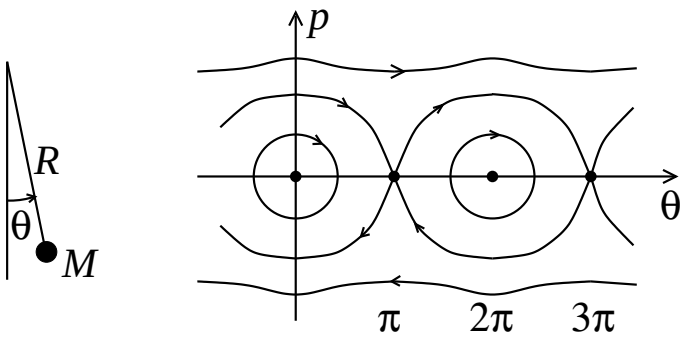

Figure 5: Phase portrait of the pendulum.

where $H = H(\mathbf{x}) \equiv H(p, q)$ is the Hamiltonian of the system. Hamilton's equations can be written in the form

$$u_i = J_{ij}\partial_j H = -\partial_j H J_{ji}, \tag{2.26}$$

where

$$\mathbf{J} = \begin{pmatrix} 0 & -1 \\ 1 & 0 \end{pmatrix} \tag{2.27}$$

is called the symplectic matrix.

We verify that the Hamiltonian flow is incompressible

$$\nabla \cdot \mathbf{u} = -\partial_p \partial_q H + \partial_q \partial_p H = 0, \tag{2.28}$$

which is the content of Louville's theorem.

If the Hamiltonian does not depend explicitly on time, the Hamiltonian flow is itself independent of time; let us take the specific example of the pendulum:

$$H = \frac{p^2}{2MR^2} - MgR\cos\theta, \qquad \theta \equiv q. \tag{2.29}$$

We show the streamlines of the flow in Fig. 5. We see that the stable equilibrium points at $\theta = 2n\pi$ correspond to regions of vortical flow, while the unstable equilibrium points at $\theta = (2n+1)\pi$ correspond to strain flow, no sinks or wells in the form described in case C of Fig. 4 are possible due to the incompressibility of the flow.

Hamilton's equations can be written in terms of Poisson brackets,

$$\dot{x}_i = \{x_i, H\}, \qquad \{f, g\} = J_{ij}\partial_i f \partial_j g \equiv \partial_p g \partial_q f - \partial_q g \partial_p f. \tag{2.30}$$

We can use the Poisson brackets to determine the variation of a field f measured by a phase point that is transported by the Hamiltonian flow $\mathbf{u}$:

$$\dot{f} = \partial_t f + \mathbf{u} \cdot \nabla f = \partial_t f + (J_{ji}\partial_j H)\partial_i f = \partial_t + \{f, H\}. \tag{2.31}$$

We can expresss energy conservation for a time-independent Hamiltonian H in the language of Poisson brackets,

$$\dot{E} \equiv \dot{H} = \{H, H\} = (J_{ji}\partial_j H)\partial_i H = 0, \tag{2.32}$$

which tells us that energy conservation is basically a consequence of the antisymmetry of the symplectic matrix $\mathbf{J}$.

We can describe the time evolution of a field frozen in a Hamiltonian flow in terms of Poisson brackets; of particular interest is the case when the frozen field is the Hamiltonian itself and the flow $\mathbf{u}^K$ are induced by an auxiliary Hamiltonian K. The result is that the original Hamiltonian is deformed, $H \to H^K$, under the law

$$\partial_t H^K = -\{H^K, K\}. \tag{2.33}$$

A trivial example is that of the pendulum in the field of the Hamiltonian $K = \Omega(t)p \Rightarrow \mathbf{u}^K = (0, \Omega(t))$. The deformed version of Eq. (2.29) would be

$$H^K = \frac{p^2}{2MR^2} - MgR\cos(\theta - \theta^K), \qquad \dot{\theta}^K = \Omega. \tag{2.34}$$

The vector field $u_i \equiv u_i^{H^K} = J_{ij}\partial_j H^K$ is itself deformed by $\mathbf{u}^K$; its dynamics is actually that of a field frozen in $\mathbf{u}_k$:

$$\begin{aligned} \dot{u}_i &= -J_{ij}\partial_j \dot{H}^K = J_{ij}\partial_j\{H^K, K\} \\ &= -J_{ij}\partial_j[J_{lm}(\partial_l H^K)\partial_m K] \\ &= -J_{ij}[u_l^K \partial_j\partial_m H^K - u_m\partial_m\partial_j K] \\ &= -u_l^K\partial_l u_i + u_m\partial_m u_i^K. \end{aligned}$$

We can write the result in terms of Lie derivatives:

$$\dot{u}_i = -\mathbf{u}^K \cdot \nabla\mathbf{u} + \mathbf{u}\cdot\nabla\mathbf{u}^K \equiv -\mathcal{L}_{\mathbf{u}^K}\mathbf{u}. \tag{2.35}$$

2.5 Suggested reading

- S. Childress, "Topological fluid dynamics for fluid dynamicists", https://www.math.nyu.edu/ childres/tfd.pdf

3 Conservation of mass and momentum

The dynamics of a fluid is described by equations that are essentially local conservation laws for the mass, the momentum, and the energy.

Conservation of mass is expressed locally by imposing the condition that the mass M_a of a fluid element is constant. We can write the condition in terms of the mass density along a fluid trajectory ρ_L and the volume V_L of the element, $M \simeq V_L \rho_L$:

$$0 = \dot{M} \simeq V_L \dot{\rho}_L + \rho_L \dot{V}_L \tag{3.1}$$

An Eulerian version of this equation can be obtained by setting in $\mathbf{x}_L(t|\mathbf{x}_0, t_0)$ and $\mathbf{v}_L(t|\mathbf{x}_0, t_0)$ the labeling time t_0 equal to t, and then using Eqs. (2.10) and (2.23) to set $\dot{\rho}_L = D_t \rho$ and $\dot{V}_L = V \nabla \cdot \mathbf{u}$. From Eq. (3.1) we thus get the continuity equation

$$D_t \rho + \rho \nabla \cdot \mathbf{u} \equiv \partial_t \rho + \nabla \cdot (\rho \mathbf{u}) = 0. \tag{3.2}$$

We see that if the flow is incompressible, the density is "frozen" in the flow; imagine an oil emulsion in water: the density $\rho(\mathbf{x}, t)$ changes in response to the passage of droplets of oil at $\mathbf{x}$ (if the fluid is in motion); however, the density $\rho_L(t)$ following the droplet remains constant.

In the absence of chemical reactions, the number density $n(\mathbf{x}, t)$ obeys an equation identical to Eq. (3.2). Otherwise, we ought to include sources and sinks in Eq. (3.2), together with separate equations for the different species; this would require taking into account the diffusion of the different species across the fluid element boundaries. Difficulties in the identification of mass and matter (molecule) fluxes also arise in a relativistic context, in which case we could interpret ρ and $\mathbf{J}_m = \rho \mathbf{u}$ as components either of a 4-current density or of a momentum density (the time components of the stress-energy tensor); to avoid this sort of trouble, we shall assume throughout the notes that relativistic effects are negligible.

The same procedure adopted in the derivation of Eq. (3.2)x, can be utilized to derive a local conservation law for the momentum; the starting point is the second law of Newton

$$M \dot{\mathbf{u}}_L(t) = \mathbf{F}(t), \tag{3.3}$$

where $\mathbf{F}$ is the force on the fluid element. If the volume V is sufficiently large, it is possible to separate in $\mathbf{F}$ a contact force component at the boundary of V. Let us consider an outward-oriented surface element $\mathrm{d}\mathbf{A}$ on the boundary of $\mathbf{V}$; we can interpret the surface force $\mathrm{d}\mathbf{F}^S$ on $\mathrm{d}\mathbf{A}$ as a momentum flux through that surface element. In the case of the flow of a scalar quantity, such as the mass, the density current is a vector $\mathbf{J}_m$; in the case of a vector, such as the force $\mathbf{F}$, the associated density current must be a second-order tensor $\boldsymbol{\sigma}$. Only in this way can $\boldsymbol{\sigma} \cdot \mathrm{d}\mathbf{A}$ bbee a vector. Indicate with σ_{ij} the momentum current density entering V, in such a way that

$$\mathrm{d}\mathbf{F}^S = \boldsymbol{\sigma} \cdot \mathrm{d}\mathbf{A}; \qquad \mathrm{d}F_i^S = \sigma_{ij} \mathrm{d}A_j. \tag{3.4}$$

The tensor $\boldsymbol{\sigma}$ is called the stress tensor of the fluid. The total force on V will be therefore

$$\mathbf{F} = \mathbf{F}^{ext} + \mathbf{F}^{A} = \mathbf{F}^{ext} + \int_{\partial V} \mathrm{d}\mathbf{A} \cdot \boldsymbol{\sigma}, \tag{3.5}$$

where $\mathbf{F}^{ext}$ is the contribution to $\mathbf{F}$ from forces mediated by long-range fields such as the gravity (note that such forces could be generated by portions of the fluid at macroscopic separations from V). We can convert the surface integral in $\mathbf{F}^{S}$ into a volume integral, $\int_{\partial V} \mathrm{d}\mathbf{A} \cdot \boldsymbol{\sigma} = \int_{V} \mathrm{d}V \, \nabla \cdot \boldsymbol{\sigma}$, and introduce force densities $\mathbf{f} = \mathbf{F}/V$ and $\mathbf{f}^{ext} = \mathbf{F}^{ext}/V$. Equation (3.5) then becomes

$$\mathbf{f} = \mathbf{f}^{ext} + \nabla \cdot \boldsymbol{\sigma}. \tag{3.6}$$

We can now substitute Eq. (3.6) into Eq. (3.3) and exploit Eq. (2.10) to switch to an Eulerian description. The the result is the conservation law for the momentum

$$\rho(\partial_t + \mathbf{u} \cdot \nabla)\mathbf{u} = \nabla \cdot \boldsymbol{\sigma} + \mathbf{f}^{ext}. \tag{3.7}$$

Proceeding as we have done with the tensor $\nabla\mathbf{u}$, when we have introduced vorticity, strain rate and compression rate, we decompose the stress tensor $\boldsymbol{\sigma}$ into its trace, symmetric zero-trace and antisymmetric components:

$$\sigma_{ij} = \frac{1}{3}\sigma_{ll}\delta_{ij} + \frac{1}{2}\Big(\sigma_{ij} + \sigma_{ji} - \frac{2}{3}\sigma_{ll}\delta_{ij}\Big) + \frac{1}{2}\Big(\sigma_{ij} - \sigma_{ji}\Big). \tag{3.8}$$

The terms in the decomposition are associated with separate contributions to the surface force on V. We see immediately that the trace component produces a force contribution $(1/3)\sigma_{ll}\mathrm{d}\mathbf{A}$ normal to the surface element, whose magnitude is independent of the orientation of $\mathrm{d}\mathbf{A}$. In other words, we are dealing with a pressure force. The symmetric traceless component contributes normal and tangential forces. The antisymmetric ones contribute only tangential forces. We see that the symmetric traceless component tends to stretch V, while the antisymmetric induces rotation of the fluid element. We illustrate the situation in Fig. 6.

Let us focus on the rotation component. As usual, indicate with a the characteristic scale of V. The contribution to $\mathbf{F}^{S}$ from the antisymmetric stress component $\sigma^{as}_{ij} = (1/2)(\sigma_{ij} - \sigma_{ji})$ has magnitude $F^{as} \sim a^2 T^{as}$. This induces a torque

$$\mathcal{T} \sim a F^{as} \sim a^3 T^{as} \tag{3.9}$$

on V. On the other hand, the inertia tensor of V is

$$I_{ij} = \int_{V} \mathrm{d}V r_i r_j \rho \sim a^5 \rho, \tag{3.10}$$

where $\mathbf{r}$ is evaluated with respect to some point in the interior of V. Comparison of Eqs. (3.9) and (3.10) tells us that T^{as} generates a response in the fluid on a time scale $I/\mathcal{T} \sim a^2$ that vanishes in the continuous limit.

Any antisymmetric component of the stress tensor that is locally generated is going to be destroyed on this time scale. We thus reach the conclusion that the stress tensor does not have an antisymmetric component.

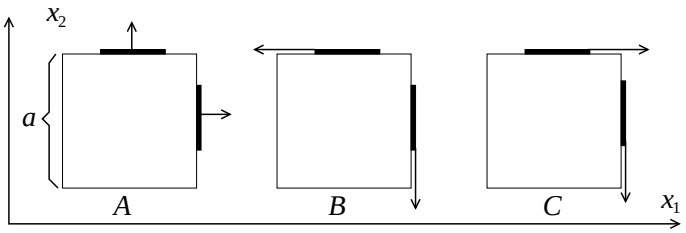

Figure 6: Examples of surface force contributions $\mathrm{d}\mathbf{F}^S$ from the trace (A), the symmetric traceless (B) and antisymmetric (C) components of the stress tensor; in the example considered, we have taken $\sigma_{11} = \sigma_{22} = \sigma_{33}$, in such a way that the diagonal terms of the symmetric traceless component are identically zero.

3.1 Suggested reading

- P. Kundu, I.M. Cohen and D.R. Dowling, "Fluid mechanics, Secs. 4.1-7 (Ac. Press 2015)
- L.D. Landau, E.M. Lifshitz, E.M. Koevich and L.P. Pitaevskii, "Theory of elasticity" Vol. 7, Secs. 1 and 2 (Elsevier, 1986)

4 Constitutive laws

The momentum conservation law Eq. (3.7) does not apply exclusively to fluids and is indeed quite general. To fix the system dynamics, we must know the dependence of the stress tensor on the density, the temperature, the fluid velocity gradient, and possibly higher-order gradients of these quantities. A relation fixing such dependency is called a constitutive law.

If the microscopic dynamics is sufficiently simple and the fluid is not too far from equilibrium, the macroscopic dynamics is local and it is possible to carry out a gradient expansion:

$$\sigma_{ij} = \sigma_{ij}^{(0)}(n,T) + \sigma_{ij}^{(1)}(n,T,\nabla\mathbf{u}) + \dots, \quad \sigma_{ij}^{(1)} = \mu_{ijlm}(n,T)\partial_l u_m. \tag{4.1}$$

If it is possible to stop the gradient expansion to the first order, we say that the fluid is Newtonian; we say that the fluid is simple if it is isotropic as well; in this case, the stress tensor has the form

$$\sigma_{ij}^{(0)} = -P\delta_{ij}, \quad \text{and} \quad \sigma_{ij}^{(1)} = \mu^B \nabla\cdot\mathbf{u}\delta_{ij} + \mu\dot{s}_{ij}, \tag{4.2}$$

where P is the pressure, and μ_B and μ define the bulk and dynamic viscosity of the fluid, since σ_{ij} is always symmetric, the stress tensor of a simple fluid is by construction independent of vorticity.

4.1 The Navier-Stokes equation

If the deviations from equilibrium of ρ and T are weak enough, it is possible in Eq. (3.7) to disrergard the variation of μ_B and μ with respect to ρ and T, and thus to approximate

$$\nabla\cdot\boldsymbol{\sigma} \simeq \mu_B\nabla\nabla\cdot\mathbf{u} + \mu\nabla\cdot\mathbf{s}.$$

The bulk viscosity of most fluids is usually small and thus disregarded; the viscous stress thus simplifies to

$$\sigma_{ij}^{(1)} = \mu\dot{s}_{ij}. \tag{4.3}$$

The momentum conservation equation (3.7) for a simple fluid becomes the Navier-Stokes equation

$$\rho(\partial_t + \mathbf{u}\cdot\nabla)\mathbf{u} + \nabla P = \mu\Big(\nabla^2\mathbf{u} + \frac{1}{3}\nabla\nabla\cdot\mathbf{u}\Big) + \mathbf{f}^{ext}. \tag{4.4}$$

In order to solve the system formed by the continuity equation (3.2) and the Navier-Stokes equation (4.4), we need in general a law of state $P = P(\rho,T)$, and an

evolution equation for the temperature. Equations (3.2) and (4.4) form a close set of equations when the flow is incompressible and the density ρ is uniform:

$$\nabla \cdot \mathbf{u} = 0, \qquad \rho(\partial_t + \mathbf{u} \cdot \nabla)\mathbf{u} + \nabla P = \mu \nabla^2 \mathbf{u} + \mathbf{f}^{ext}, \tag{4.5}$$

in which case the pressure is fixed by the incompressibility constraint.

An analytical solution of the Navier-Stokes equation is not possible in general because of the equation's nonlinearity; the strength of the nonlinearity is determined by the relative magnitude of the advection and viscous terms:

$$\mathbf{u} \cdot \nabla \mathbf{u} \sim \frac{(\delta u)^2}{L}, \qquad \nu \nabla^2 \mathbf{u} \sim \frac{\nu \delta u}{L^2}. \tag{4.6}$$

Out of the quantities in Eq. (4.6) we can form a dimensionless quantity called the Reynolds number

$$\mathrm{Re} = \frac{L \delta u}{\nu}. \tag{4.7}$$

The dynamics of a large Reynolds number flow is the result of a balance between the pressure and external forces, and the inertia of the fluid—the latter contribution accounted for by $\rho D_t \mathbf{u}$. Now, at large Re, a fluid flow will typically be turbulent, which means that a multiplicity of space and velocity scales are present in the flow. There will thus be a multiplicity of scale-dependent Reynolds numbers

$$\mathrm{Re}_l = \frac{l \delta_l u}{\nu}, \tag{4.8}$$

giving the relative strength of inertia and viscous forces at the different flow scales.

In the case of a turbulent flow, the scale L and the characteristic velocity $\delta u \equiv \delta_L u$ correspond to the scale of the largest eddies, determined by the boundary conditions of the flow (say, the width of a duct). Typically, Re_l is an increasing function of l, so that $\mathrm{Re} \equiv \mathrm{Re}_L = \max_l \mathrm{Re}_l$.

4.2 Condition of local thermodynamic equilibrium

The law of state $P = P(\rho, T)$ and the functional form of the viscosity coefficient $\mu = \mu(\rho, T)$ both depend on the microscopic characteristics of the fluid.

Considering the fluid in conditions not too far from equilibrium basically means that concepts from equilibrium thermodynamics, such as, e.g., the temperature, at least locally, continue to apply. Local thermodynamic equilibrium is only possible if the fluid is homogeneous at the scale of the mean-free path λ; the latters is typically longer than the molecule separation. Relaxation processes at the molecular scale would not be able to smooth out variations of macroscopic quantities at scales below λ. The condition of slow space variation of macroscopic quantities, in turn, requires that the macroscopic dynamics is sufficiently slow to give time to the relaxation

processes to be effective; thus, the macroscopic dynamics must not be too violent (say, a detonation) or take place at scales below that of the mean free path.

The magnitude of the mean free path λ is determined by the geometry of the collision process. Let r_0 be the characteristic size of a molecule; the molecular volume is the typical volume in the gas (or liquid) containing just one molecule, which is $\sim n^{-1} \equiv a_0^3$. The cross-section of a molecule is r_0^2; the probability that a second molecule crossing the molecular volume of the first one, actually hits it, is, therefore, $\sim (r_0/a_0)^2$. Typically, a molecule will have to cross $\sim (a_0/r_0)^2$ molecular volumes, each of length a_0, before making a collision. The total distance traveled defines the mean free path

$$\lambda = a_0^3/r_0^2 = \frac{1}{nr_0^2}. \tag{4.9}$$

The condition of local thermodynamic equilibrium can be expressed in terms of the so-called Knudsen number

$$\mathrm{Kn} = \frac{\lambda}{l} \sim \frac{1}{nr_0^2 l} \ll 1. \tag{4.10}$$

Since $\lambda \geq a_0$, the condition for local thermodynamic equilibrium $l \gg \lambda$ is stronger than the one for the continuum $l \gg a_0$, discussed in Sec. 1.

4.2.1 Digression into plasma physics

An example of a system for which the continuum limit is satisfied, but local equilibrium is difficult, is that of hot plasmas.

Due to the long-range nature of electromagnetic interactions, the collision cross-section r_0 of the charged particles in a plasma is not well defined; a possibility is to introduce the concept of "hard" collision, as a scattering event involving a substantial change of direction in the motion of the particles; this requires that when the particles are at their minimum separation, their kinetic and potential energy are of the same order:

$$mv^2 \sim \frac{e^2}{r(v)}, \tag{4.11}$$

where v is the relative velocity of the incoming particles, e is their charge and m is the reduced mass (for a typical plasma, in which the lighter particles are the electrons, m is the electron mass).

We can identify the parameter $r(v) = e^2/(mv^2)$ as the effective interaction radius of the particles at relative velocity v. By taking $r_0 \sim r(v_{th})$, with v_{th} the thermal velocity of the electrons, we get the estimate of the mean free path

$$\lambda = \frac{1}{nr_0^2} \sim \frac{1}{n}\Big(\frac{mv_{th}^2}{e^2}\Big)^2 \sim n\Big(\frac{k_B T}{e^2}\Big)^2, \tag{4.12}$$

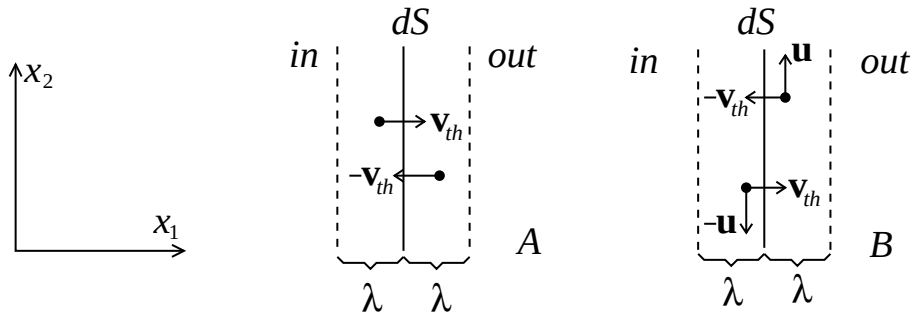

Figure 7: Sketch of the microscopic mechanisms responsible for pressure (A) and viscous (B) forces at the surface of a fluid element; all velocities measured in the reference frame of d$\mathbf{A}$.

where k_B is Boltzmann constant.

We point out that for our estimate to be correct, the plasma must be sufficiently dilute for binary collisions to be dominant; in other words, the plasma must be weakly correlated. This requires $r_0 \ll a_0$, which together with the continuous limit condition $nl^3 \gg 1$ implies

$$\frac{k_B T}{e^2} \gg n^{1/3} \gg l^{-1}. \tag{4.13}$$

A plasma may satisfy the continuum and weak correlation conditions in Eq. (4.13); however, if its temperature is too high, the effective Knudsen number λ/l may be so large that local thermal equilibrium is impossible; such a hot plasma would not admit a fluid description.

4.3 Microscopic interpretation of pressure and viscosity

The condition Kn $\ll 1$ allows us to describe the pressure and viscous forces acting on a fluid element Va, as the result of a process of deposition of momentum by the molecules crossing the boundary of V; the process takes place in a layer of thickness λ at the boundary of the fluid element, as described in Fig. 7.

Case A of Fig. 7 illustrates the production mechanism for pressure in the case of a homogeneous gas; molecules to the right of dA travel left with a velocity $-\mathbf{v}_{th}$ and deposit momentum $-m\mathbf{v}_{th}$ in the layer of thickness λ to the left of dA (consider for simplicity the case of a single molecule species). At the same time, molecules on the left travel right with velocity $\mathbf{v}_{th}$ and deposit momentum $m\mathbf{v}_{th}$ out of V, thus contributing other $-m\mathbf{v}_{th}$ to the balance for V; the current from right to left and the one from left to right have magnitude $\sim nv_{th}\mathrm{d}A/2$ (one-half of the molecules to the right travel to the left, and one-half of those to the left travel to the right. The total flow of momentum to the left, which is the portion of the normal component

of $\mathbf{F}^S$ exerted on $\mathrm{d}A$, is $\mathrm{d}F^\perp \sim nmv_{th}^2 \mathrm{d}A$, from which we get the law of state

$$P \sim nmv_{th}^2 \sim nK_BT, \tag{4.14}$$

where k_B is Boltzmann constant. We could turn the order of magnitude relation to an equality by a more careful analysis based on kinetic theory.

The mechanism for viscous forces is illustrated in Fig. 7*B*. We are interested in this case in the tangential forces produced by the transfer of vertical momentum across $\mathrm{d}A$.

Suppose that there is a horizontal gradient $\partial_1 u_2 > 0$. Molecules that have equilibrated at distance λ to the right of $\mathrm{d}A$ will have average vertical momentum $m\lambda\partial_1 u_2$. The molecule current from right to left will be, as before, $\sim nv_{th}\mathrm{d}A/2$. At the same time molecules that have equilibrated at distance λ to the left of $\mathrm{d}A$ will have average vertical momentum $-m\lambda\partial_1 u_2$ and the current to the right will be $\sim nv_{th}\mathrm{d}A/2$. The total flow of momentum to the left, which is the portion of the tangential component of $\mathbf{F}^S$ exerted on $\mathrm{d}A$, will be therefore

$$\mathrm{d}F^\parallel \sim nmv_{th}\lambda\partial_1 u_2 \mathrm{d}A, \tag{4.15}$$

corresponding to the viscous stress

$$\sigma_{12} = \mu\partial_1 u_2, \qquad \mu \sim nmv_{th}\lambda \sim \frac{mv_{th}}{r_0^2}. \tag{4.16}$$

The dynamic viscosity of a gas is independent of its density; experimental verification of this fact by J.C. Maxwell provided the first evidence in support of the kinetic theory of gases. A parameter often used in place of the dynamic viscosity is the kinematic viscosity

$$\nu = \mu/\rho \sim \lambda v_{th}. \tag{4.17}$$

For water $\nu \simeq 0.01\,\mathrm{cm}^2/\mathrm{s}$; for air at sea level $\nu \simeq 0.15\,\mathrm{cm}^2/\mathrm{s}$.

A mechanism similar to the one we have discussed in the case of viscosity, is at play with heat diffusion, and is illustrated in Fig. 8. Suppose $\partial_1 T > 0$; this means $T' \simeq T - \lambda\partial_1 T$ and $T'' \simeq T + \lambda\partial_1 T$, and therefore also $v'_{th} \simeq v_{th} - (v_{th}/(2T))\lambda\partial_1 T$ and $v''_{th} \simeq v_{th} - (v_{th}/(2T))\lambda\partial_1 T$. At the same time, equilibrium of pressure forces requires $n'T' = n''T'' = nT$. The heat current density to the right is $\sim n'v'_{th}k_BT'/2 = nv'_{th}k_BT/2$ and the one to the left is $\sim -n''v''_{th}k_BT''/2 = -nv''_{th}k_BT/2$. The total heat current density along x_1 is therefore

$$q_1 \sim nk_BT(v'_{th} - v''_{th})/2 \sim -\kappa n k_B \partial_1 T, \qquad \kappa \sim \lambda v_{th}. \tag{4.18}$$

The diffusivity κ is typically of the same order of the kinematic viscosity ν.

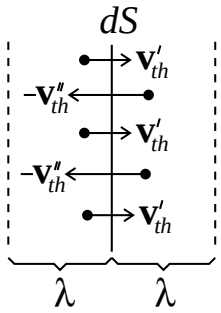

Figure 8: Mechanism for the generation of a heat flux. A positive temperature gradient is present such that $v''_{th} > v'_{th}$ and at the same time $n'' < n'$, in such a way that $P'' = P'$. But this implies $n'v'^3_{th} < n''v''^3_{th}$, which means that there is a heat flux to the left.

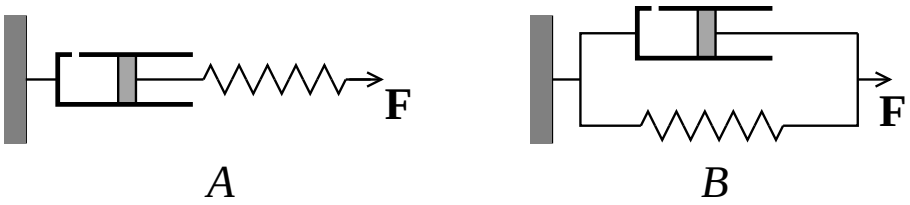

Figure 9: Mechanical analogs of a Maxwell fluid (A) and of a Kelvin-Voigt solid (B).

4.4 Non-Newtonian fluids

Non-Newtonian fluids comprise a vast zoo of behaviors. Some materials are characterized by a viscosity coefficient that depends on the magnitude of the strain rate. The viscosity of these materials may increase with s (shear-thickening materials, such as corn starch) or decrease with s (shear-thinning materials, such as sand in water). In some cases, memory effects may be present, and the viscosity may depend on the duration of the stress.

Other continuous media are characterized by a stress tensor depending on the strain rate and the strain. We speak in this case of viscoelastic materials. We can distinguish two main classes: materials in which the elastic component of the stress is generated as a transient, and the steady-state dynamics is dominated by the viscous stress; materials in which viscous stresses are significant in the transient, and the steady-state is dominated by elastic forces. Materials in the first class are called Maxwell fluids (or solid-like fluids); materials in the second class are called Kelvin-Voigt solids (or fluid-like solids). Examples in the first class include whipped cream, mucus, the silly putty; the second class we find living tissues and some plastics. A mechanical analog of the dynamics of Maxwell fluids and Kelvin-Voigt solids is illustrated in Fig. 9.

It is interesting to note that the elastic stress of a solid and the viscous stress of a fluid have the same functional form, with the compression $\nabla \cdot \mathbf{y}$ replacing the compression rate $\nabla \cdot \mathbf{u}$ and the strain $s_{ij} = \partial_i y_j + \partial_j y_i - (2/3)\nabla \cdot \mathbf{y}\delta_{ij}$ replacing the strain rate $\dot{s}_{ij} = \partial_i u_j + \partial_j u_i - (2/3)\nabla \cdot \mathbf{u}\delta_{ij}$, where $\mathbf{y}(t|\mathbf{x}_0) = \mathbf{x}_L(t|\mathbf{x}_0) - \mathbf{x}_0$ is the dislocation of the solid element with equilibrium coordinate $\mathbf{x}_0$.

The mechanical analogs in Fig. 9 allow us to derive constitutive laws for Maxwell and Kelvin-Voigt materials. The spring and the friction-generating piston-cylinder assembly in the figure, could be seen as the microscopic components responsible for the stress at the surface of a fluid element, all assumed to have zero inertia.

In the case of a Maxwell material, the friction and the spring act in series; at steady-state, the spring reaches the equilibrium elongation corresponding to the friction force on the moving piston. In the case of a Kelvin-Voigt material, the two forces act in parallel; at steady-state, the spring reaches the equilibrium elongation corresponding to the external forces $\mathbf{F}$ on the assembly, while the friction force is zero.

Identify with subscript S and P the spring and piston components of stress, strain and rate of strain. In the Maxwell case, the stress is constant along the chain (because of zero inertia). Hence

$$\sigma = \alpha s_A = \mu \dot{s}_P, \quad s_A + s_P = s \quad \Rightarrow \quad \dot{s} = \frac{\dot{\sigma}}{\alpha} + \frac{\sigma}{\mu}, \tag{4.19}$$

where α plays the role of elasticity modulus (Lamé coefficient) of the material. In the Kelvin-Voigt case, the deformations of the spring and the cylinder-piston assembly are equal. Total stress is the sum of the two components

$$s_A = s_P = s \quad \Rightarrow \quad \text{and} \quad \sigma = \sigma_A + \sigma_P = \alpha s + \mu \dot{s}. \tag{4.20}$$

4.5 Suggested reading

- P. Kundu, I.M. Cohen and D.R. Dowling, "Fluid mechanics, Secs. 4.8-9 (Ac. Press 2015)

5 Conservation of energy

The continuity equation (3.2) and the Navier-Stokes equation (4.4), together with the constitutive laws Eqs. (4.14) and (4.16), do not form a closed system. An additional equation for the temperature must be provided. We obtain such an equation by imposing energy conservation and separating the contributions from the kinetic energy and the internal energy of the fluid.

5.1 Kinetic energy balance

An equation for the kinetic energy can be obtained in general form by taking the scalar product of Eq. (3.7) with $\mathbf{u}$:

$$(1/2)\rho D_t u^2 = \mathbf{u}\cdot(\nabla\cdot\boldsymbol{\sigma} + \mathbf{f}^{ext}). \tag{5.1}$$

We exploit the continuity equation (3.2) to write Eq. (5.1) as

$$D_t(\rho u^2/2) = -\rho u^2\nabla\cdot\mathbf{u}/2 + \mathbf{u}\cdot(\nabla\cdot\boldsymbol{\sigma} + \mathbf{f}^{ext}). \tag{5.2}$$

We note the advection term $-\rho u^2\nabla\cdot\mathbf{u}/2$ to RHS of the equation, which does contribute to the balance of kinetic energy $K_L = \int_{V_L} \mathrm{d}V\rho u^2/2$ in a volume V_L following the fluid. Such a term is not present in Eq. (3.7), because of the condition of zero momentum advection into a fluid element, $\int_{S_L}\mathrm{d}\mathbf{A}_L\cdot\mathbf{u} = \int_{V_L}\mathrm{d}V\nabla\cdot\mathbf{u} = 0$.

We exploit Eqs. (4.2) and (4.3) to write explicitly

$$-\boldsymbol{\sigma} : (\nabla\mathbf{u}) = P\nabla\cdot\mathbf{u} - \mu\dot{s}_{ij}\partial_i u_i = P\nabla\cdot\mathbf{u} - (\mu/2)||\dot{\mathbf{s}}||^2/2, \tag{5.3}$$

where $||\dot{\mathbf{s}}||^2 \equiv s_{ij}s_{ij}$. We substitute into Eq. (5.2) and we get

$$\begin{aligned}\partial_t(\rho u^2/2) &= \nabla\cdot(\boldsymbol{\sigma}\cdot\mathbf{u} - \rho u^2\mathbf{u}/2) - \boldsymbol{\sigma}\cdot(\nabla\mathbf{u}) + \mathbf{u}\cdot\mathbf{f}^{ext}\\ &= \nabla\cdot(\boldsymbol{\sigma}\cdot\mathbf{u} - \rho u^2\mathbf{u}/2) + P\nabla\cdot\mathbf{u} - \mu||\dot{\mathbf{s}}||^2/2 + \mathbf{u}\cdot\mathbf{f}^{ext},\end{aligned}$$

which, integrated over a fixed volume V, yields the balance equation for the kinetic energy in the volume, $K = (1/2)\int_V \mathrm{d}V\rho u^2$:

$$\dot{K} = \int_{\partial V}\mathrm{d}\mathbf{A}\cdot[\boldsymbol{\sigma}\cdot\mathbf{u} - \rho u^2\mathbf{u}/2] + \int_V \mathrm{d}V\,[P\nabla\cdot\mathbf{u} - \mu||\dot{\mathbf{s}}||^2/2 + \mathbf{u}\cdot\mathbf{f}^{ext}]. \tag{5.4}$$

The surface integral to RHS of the equation accounts for the kinetic energy flow into V produced by advection and for the work by the stress forces on S. The first two terms in the volume integral describe the conversion of kinetic energy into internal energy through compression and viscous dissipation. The contribution by viscous dissipation is always negative. Thus, if the fluid is in a tank with fixed walls, it is incompressible, and $\mathbf{f}^{ext} = 0$, $\dot{K}$ will be negative and any initial motion in the fluid will come to a halt.

5.2 Heat transport

Let us indicate with $\mathcal{E}$ the internal energy per unit mass of the fluid. The total energy in a fluid element V_L will be therefore

$$E_L \simeq V_L \rho (u_L^2/2 + \mathcal{E}_L) = M(u_L^2/2 + \mathcal{E}_L). \tag{5.5}$$

A balance equation for E_L must take into account the work contribution from $\mathbf{f}^{ext}$ and $\boldsymbol{\sigma}$, as well from possible heat fluxes $\mathbf{q}$ out of the volume and heat sources h^{ext} in it. We can exploit Eq. (2.10) and write for $\dot{E}_L = M(\mathrm{d}/\mathrm{d}t)(u_L^2/2 + \mathcal{E}_L)$:

$$\begin{aligned} M D_t(u^2/2 + \mathcal{E}) &= V(\mathbf{u}\cdot\mathbf{f}^{ext} + \rho h^{ext}) + \int_{\partial V} \mathrm{d}\mathbf{A}\cdot(\mathbf{u}\cdot\boldsymbol{\sigma} - \mathbf{q}) \\ &= V[\mathbf{u}\cdot\mathbf{f}^{ext} + h^{ext} + \nabla\cdot(\mathbf{u}\cdot\boldsymbol{\sigma}) - \nabla\cdot\mathbf{q}], \end{aligned}$$

which becomes, after subtraction of Eq. (5.1),

$$\begin{aligned} \rho D_t\mathcal{E} + \nabla\cdot\mathbf{q} &= \nabla\cdot(\mathbf{u}\cdot\boldsymbol{\sigma}) - \mathbf{u}\cdot(\nabla\cdot\boldsymbol{\sigma}) + \rho h^{ext} \\ &= \boldsymbol{\sigma} : (\nabla\mathbf{u}) + h^{ext}, \end{aligned}$$

and then, by exploiting again Eq. (5.3),

$$\rho D_t\mathcal{E} + P\nabla\cdot\mathbf{u} = -\nabla\cdot\mathbf{q} + \mu||\dot{\mathbf{s}}||^2/2 + \rho h^{ext}. \tag{5.6}$$

We can convert the heat transport equation (5.6) into an equation for the temperature. Suppose that the fluid is quiescent, in such a way that any change of temperature in the fluid element is the result of heating. We can thus write

$$\rho \mathrm{d}\mathcal{E} = \rho h^{ext}\mathrm{d}t = n c_V k_B \mathrm{d}T, \tag{5.7}$$

where c_V is the specific heat per molecule at constant volume (in the case of a gas of monoatomic molecules, $c_V = 3/2$). Equation (5.6) then takes the form

$$n c_V k_B D_t T + P\nabla\cdot\mathbf{u} = -\nabla\cdot\mathbf{q} + \mu||\dot{\mathbf{s}}||^2/2 + \rho h^{ext}. \tag{5.8}$$

In order for Eqs. (3.2), (4.4) and (5.6) to form a closed system, we still need constitutive equations for the pressure and the heat flux. In the case of a gas, the pressure obeys the law of state Eq. (4.14), and the constant c_V is usually reabsorbed in the definition of the diffusivity κ (see Eq. (4.18)):

$$\mathbf{q} = -n\kappa c_V k_B \nabla T := -\hat{\kappa}\nabla T. \tag{5.9}$$

As previously done with the viscosity, effects from the variation of $\kappa\rho$ are disregarded, and Eq. (5.6) takes the final form

$$D_t T + \frac{1}{c_V} T\nabla\cdot\mathbf{u} = \kappa\nabla^2 T + \frac{1}{c_V k_B}[\nu||\dot{\mathbf{s}}||^2/2 + m h^{ext}]. \tag{5.10}$$

5.3 Isoentropic flow

We can apply Eq. (5.6) to study the evolution of the internal energy content E_L of a volume of fluid V_L (non necessarily a fluid element) transported by the flow. Equation (2.23) and mass conservation allows us to write $\int_V \mathrm{d}V\,(\rho D_t\mathcal{E} + P\nabla\cdot\mathbf{U}) = \dot{E}_L + P\dot{V}$, from which we get

$$\dot{E}_L + P\dot{V}_L = H, \tag{5.11}$$

where

$$H = -\int_{\partial V} \mathrm{d}\mathbf{A}\cdot\mathbf{q} + \mu\int_V \mathrm{d}V\,[||\dot{\mathbf{s}}||^2/2 + \rho h^{ext}]. \tag{5.12}$$

We recognize in Eq. (5.11) the first law of thermodynamics applied to the fluid element V_L. Correspondingly, the sum of the integrated entropy flux and the total entropy production is

$$\dot{S}_L = \int_V \mathrm{d}V\,\frac{-\nabla\cdot\mathbf{q} + \mu||\dot{\mathbf{s}}||^2 + \rho h^{ext}}{T}. \tag{5.13}$$

By substituting Eq. (5.9) into Eq. (5.13), we can verify that the entropy of an isolated system does not decrease with time, which is the content of the second principle of thermodynamics. In the case of an isolated system, we have in fact

$$\begin{aligned}
\dot{S}_L &= \int_V \mathrm{d}V\,T^{-1}[\hat{\kappa}\nabla^2 T + \mu||\dot{\mathbf{s}}||^2] \\
&\leq \hat{\kappa}\int_V \mathrm{d}V\left[\nabla\cdot\frac{\nabla T}{T} - \nabla T\cdot\nabla\frac{1}{T}\right] \\
&= -\int_{A_L}\mathrm{d}\mathbf{A}\cdot\mathbf{q} + \hat{\kappa}\int_{V_L}\mathrm{d}V\,\frac{|\nabla T|^2}{T^2},
\end{aligned} \tag{5.14}$$

which tells us that in the absence of external heat fluxes, $\dot{S}_L \geq 0$.

If the entropy S_L of fluid elements is conserved along a fluid trajectory, also the entropy density $s_L = S_L/M$ will be conserved, and the entropy density $s(\mathbf{x},t)$ will be a frozen field

$$D_t s = 0. \tag{5.15}$$

If s is conserved along the flow, an initially uniform distribution of s will remain uniform also at later times; we say in this case that the flow is isoentropic.

In isoentropic conditions, values of ρ and T along a fluid trajectory are related by an adiabatic transformation. From Eqs. (2.23) and (5.8) we have in fact

$$n\rho c_V k_B D_t T = P D_t\rho \quad\Rightarrow\quad \rho^2\frac{\mathrm{d}T}{\mathrm{d}\rho} = \frac{m}{c_V k_B}P(\rho,T), \tag{5.16}$$

which is replaced, in the case of a gas for which $P = nk_BT$, by the familiar relation

$$\rho \frac{\mathrm{d}T}{\mathrm{d}\rho} = \frac{T}{c_V} \Rightarrow T\rho^{-1/c_V} = C, \tag{5.17}$$

where C is constant throughout the fluid.

Equation (5.16) implies

$$P = P(\rho, T(\rho)). \tag{5.18}$$

A flow such that the pressure only depends on the density is said to be barotropic. Surfaces at constant pressure, in a barotropic flow, coincide with those at constant density, and therefore, through the law of state also with those of constant temperature.

5.4 Propagation of sound

We can use conservation laws Eqs. (3.2), (4.4) and (5.10), together with the law of state Eq. (4.14), to obtain the dispersion relation for sound waves in a gas.

Let us take the direction of propagation of the wave along x_1; we write the density, the pressure, and the temperature as sums of an equilibrium part and a fluctuation:

$$\rho = \bar{\rho} + \tilde{\rho}, \quad T = \bar{T} + \tilde{T}, \quad P = \bar{P} + \tilde{P}. \tag{5.19}$$

In the reference frame of the fluid, of course, $\mathbf{u} = \tilde{\mathbf{u}} = (u, 0, 0)$. For lighter notation, we drop index 1 on vector components.

We linearize Eqs. (3.2) and (4.4) with respect to fluctuations, and disregard in (4.4) viscous and external forces. We get

$$\partial_t \tilde{n} + \bar{n}\partial_x u = 0, \tag{5.20}$$

$$\bar{\rho}\partial_t \tilde{u} + \partial_x \tilde{P} = 0. \tag{5.21}$$

We neglect in the heat equation (5.10) all contributions from heat source and heat fluxes, which means that we are in an adiabatic regime. We use the law of state $P = (k_B/m)\rho T$ to write Eq. (5.17) in terms of pressure and density

$$\mathrm{d}P = \frac{c_P P}{c_V \rho}\mathrm{d}\rho \Rightarrow \tilde{P} = \frac{c_P k_B \bar{T}}{c_V m}\tilde{\rho}, \tag{5.22}$$

where $c_P = 1 + c_V$ is the specific heat per molecule at constant pressure.

Solution of Eqs (5.20-5.22) yields d'Alambert's equation

$$(\partial_t^2 - c_s^2 \partial_x^2)\tilde{P} = 0, \tag{5.23}$$

where

$$c_S = \sqrt{\frac{c_P k_B \bar{T}}{c_V m}} \sim v_{th} \tag{5.24}$$

is the sound propagation speed.

The solution of Eq. (5.23) are sinusoidal waves $\propto \exp(k(x - c_s t))$. We evaluate the magnitude of the nonlinearity correction in the Navier-Stokes equation

$$\frac{u\partial_x u}{\partial_t u} \sim \frac{ku^2}{\omega u} = \frac{u}{c_s} \sim \frac{u}{v_{th}}. \tag{5.25}$$

Nonlinear advection is important for $u \sim v_{th}$, and we can verify from Eqs. (5.20) and (5.21) that in this regime $\tilde{P} \sim \bar{P}$ and $\tilde{\rho} \sim \bar{\rho}$. This means that in the nonlinear regime, cavitation phenomena, in which $\rho = 0$ in the troughs of the wave, become possible.

Let us now determine the magnitude of the viscous correction. We find from Eq. (4.4)

$$\frac{\nu\partial_x^2 u}{\partial_t u} \sim \frac{\nu k^2}{\omega} = \frac{\nu\omega}{c_s^2}. \tag{5.26}$$

For $\nu \simeq 0.15\,\mathrm{cm}^2/\mathrm{s}$ and $c_s \simeq 340\,\mathrm{m/s}$, we find that in order for viscous effects to be important, we would need $\omega \sim 10^8\,\mathrm{Hz}$, which is an astonishingly high frequency. Exceedingly high frequency would be required as well for diffusion to be so large to invalidate the adiabatic approximation in Eq. (5.22).

5.5 Bernoulli's equation

For zero viscosity, the Navier-Stokes equation (4.4) is replaced by

$$\rho D_t \mathbf{u} + \nabla P = \mathbf{f}^{ext}, \tag{5.27}$$

which is called Euler's equation. In barotropic conditions, $\mathrm{d}P/\rho = \mathrm{d}P(\rho)/\rho$ is an exact differential that we indicate with w, and which is identified with the enthalpy density of the fluid. If $\mathbf{f}^{ext}/\rho = \mathbf{F}^{ext}/M$ can be derived by a potential, $\mathbf{f}^{ext}/\rho = -\nabla\Psi$, we can rewrite Euler's equation as

$$D_t \mathbf{u} + \nabla(w + \Psi) = 0. \tag{5.28}$$

By scalar multiplication of Eq. (5.28) with $\mathbf{u}$, we obtain an energy balance equation, which, in the case of a time-independent flow, takes a particularly simple form:

$$\mathbf{u} \cdot \nabla\left(\frac{u^2}{2} + w + \Psi\right) = 0. \tag{5.29}$$

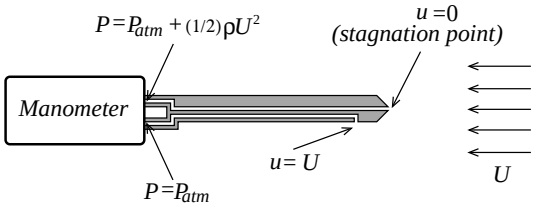

Figure 10: Schematics of the Pitot pipe

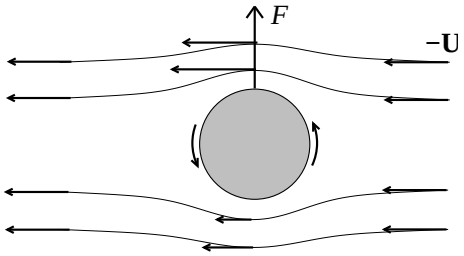

Figure 11: The Magnus effect.

By integrating Eq. (5.29) along a field line, we obtain Bernoulli's equation

$$\frac{u^2}{2} + w + \Psi = \text{constant}. \tag{5.30}$$

Of particular interest is the case the flow is incompressible and $\Psi = gx_3$ is the gravitational potential. Of course, an incompressible flow can be time-independence only if ρ is constant in space. Equation (5.30) reads in this case

$$\frac{1}{2}\rho u^2 + P + \rho g x_3 = \text{constant}, \tag{5.31}$$

which is the original form Bernoulli derived his equation in 1738.

The physical content of Bernoulli's equation is that the pressure of a fluid flowing at a constant height increases where it down and decreases where it accelerates; in the case the height of the fluid changes during the motion, the pressure and the kinetic energy must compensate for the change in potential energy.

The Pitot pipe is an example of a device that works thanks to Bernoulli's law. We illustrate the mechanics of the device in Fig. 10. The Pitot pipe allows one to determine the flow velocity of the fluid from the pressure difference generated in two channels: one facing the flow, in the so-called stagnation point, where the fluid velocity is zero, the other tangent to the flow, where the fluid velocity is approximately equal to its value far from the device.

Another application of Bernoulli's equations is the explanation of the Magnus effect. This is the effect that allows a football player, by giving a ball a spin, to have the ball follow a curved trajectory. We illustrate the idea in Fig. 11, which

represents a ball flying to the right with velocity $\mathbf{U}$, spinning counterclockwise, and consequently subjected to an upwards lift force $\mathbf{F}$.

In the reference frame of the ball, the air approaches the ball with speed $-\mathbf{U}$; when it gets close, however, it slows down and tends to be dragged along by the surface of the spinning ball. The air on top of the ball will flow faster than the air below; by Bernoulli's equation, the velocity decrease of the air along its streamlines must be compensated by an increase of the pressure, which the strongest under the ball; the result is a lift force $\mathbf{F}$ pushing the ball upwards.

The explanation of the Magnus effect provided by Bernoulli's equation has several limitations. In the first place, the air, to feel the drag by the rotating ball, must have finite viscosity. This, however, violates the hypothesis at the basis of Bernoulli's equation, that the flow is inviscid; a second difficulty is that the flow near the ball becomes turbulent and thus cannot be considered stationary, which is problematic, as the drag force on the ball induced by turbulence may have a lateral component and hence contribute to the lift.

Limitations in the applications of Bernoulli's equation, similar to the one just discussed, arise in several contexts; as a rule of thumb, Bernoulli's equation approach allows one to obtain a qualitative understanding of a process but often fails short when the goal are quantitative estimates.

5.6 Suggested reading

- L.D. Landau and E.M. Lifshitz, "Fluid mechanics" Vol. 6, Secs. 2, 5, 6 and 16 (Pergamon Press 1987)

- P. Kundu, I.M. Cohen and D.R. Dowling, "Fluid mechanics, Secs. 4.12-16 (Ac. Press 2015)

6 Hydrostatics

A fluid in equilibrium conditions obeys hydrostatic balance

$$\nabla P = \mathbf{f}^{ext}, \tag{6.1}$$

which descends straightforwardly from the Navier-Stokes equation (4.4). Equation (6.1) is the content of Pascal's principle, which states that at equilibrium there must be a balance between pressure forces and external forces in the fluid. The solution of Eq. (6.1) is called the hydrostatic pressure.

We focus again on the case in which $\mathbf{f}^{ext} = -\rho g \mathbf{e}_3$ is the gravitational force. In the case the fluid density is constant, as in the case of water, Eq. (6.1 can be integrated to give

$$P(x_3) = P(0) - x_3 \rho g, \tag{6.2}$$

which is called Stevino's law. Combining Stevino's law and Bernoulli's equation allows us to derive Torricelli's law, which gives the flow velocity of water out of an orifice in a tank as a function of the height h of the water column above the orifice. The pressure at the water surface and outside the orifice equals the atmospheric pressure P_{atm} (in this and the following examples, we disregard the change of P_{atm} at the scales under consideration); inside the tank, the pressure at the level of the orifice, from Eq. (6.2), equals $P_{atm} + \rho g h$, and the fluid velocity is zero. Bernoulli's equation (5.31) then implies $P_{atm} + \rho g h = P_{atm} + (1/2)\rho u^2$, where u is the flow velocity just out of the orifice. From here, we get Torricelli's law

$$u = \sqrt{2gh}. \tag{6.3}$$

Stevino's law implies the law of communicating vessels, which states that the water level in the vessels must be identical at equilibrium. The proof is straightforward: if P_0 is the pressure in a point of the fluid at height $x_{3,0}$, and $x_{3,a}$ and $x_{3,b}$ are the water levels in vessels a and b, the pressure at the water surface in the two vessels will be $P_a = P_0 - (x_{3,a} - x_{x_0})\rho g$ and $P_b = P_0 - (x_{3,b} - x_{x_0})\rho g$. However, since at equilibrium $P_a = P_b = P_{atm}$, we must also have $x_{3,a} = x_{3,b}$. For the same reason, at equilibrium, the water surface in a tank must be horizontal.

Pascal's law explanains how lifting and pressing devices work; we illustrate the mechanism in Fig. 12. The pressure on a and b, subtracted of the hydrostatic contribution $\rho g(x_{3,a} - x_{3,b})$, must be equal. The force on a required to lift the weight M on b is therefore

$$F_a = \frac{A_b}{A_a} M g, \tag{6.4}$$

where A_a and A_b are the areas of the pistons in a and b.

The same principle behind the hydraulic lift has a spectacular realization in an experiment Pascal himself proposed: suppose that a barrel is communicating at the

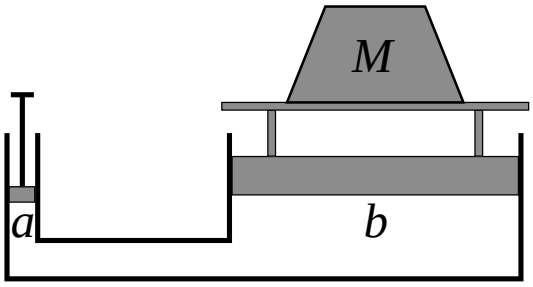

Figure 12: Mechanism of the hydraulic lift.

top with a thin and long vertical pipe and that the whole assembly is water-tight; pour water until barrel and pipe are both full; the pressure at height x_3 in the barrel is $P = P_{atm} + (h - x_3)\rho g$, where h is the length of the pipe. We then see that if h is sufficiently large, the pressure P will eventually cause the barrel to crack open. The remarkable fact is that the result is independent of the pipe radius (and therefore of the amount of water in the pipe).

Another physical law that can be derived from Eq. (6.1) is Archimedes' principle: an immersed body is subjected to a lift force equal to the weight of the displaced water. Indicate with A_w and A_a, $A = A_w \cup A_a$, the portions of the body surface below and above the water surface, and with $\mathrm{d}\mathbf{A}$ the surface-element oriented out of the body. Let us put the origin of the axes at the water surface, pointing upwards; the lift force on the body is

$$\begin{aligned} F_3 &= -\int_A \mathrm{d}A_3 P(x_3) = -P_{atm}\int_{A_a}\mathrm{d}A_3 - \int_{A_w}\mathrm{d}A_3(P_{atm} - g\rho x_3) \\ &= g\rho\int_{A_w}\mathrm{d}A_3 x_3 = g\rho V_w, \end{aligned} \tag{6.5}$$

where V_w is the underwater portion of the body, and where to reach the result we have exploited $\int_A \mathrm{d}\mathbf{A} = 0$.

6.1 Stability under convection

We can apply the hydrostatic balance condition Eq. (6.1) to describe the stability properties of an air column subjected to earth's gravity. The equation takes the form

$$\partial_3 P = -g\rho, \tag{6.6}$$

where the density ρ now is not constant. For the volume to be in equilibrium, P must be horizontally uniform, which implies through Eq. (6.6) and the law of state $P = (k_B/m)\rho T$, that also ρ and T are horizontally uniform; in other words, the air is in barotropic conditions; the vertical profiles of P, ρ and T, however, remain

undetermined, with different vertical profiles corresponding to different stability properties of the air column.

Instability occurs if the vertical displacement of a volume of air results in a density gap with the surroundings, generating a buoyancy lift in the direction of the displacement; conversely, the column is stable if such a displacement generates a buoyancy force in a direction opposite to the displacement. Instability is expected in the presence of large negative vertical temperature gradients in the column: a rising volume of hot air near the ground will find itself in regions where the air is colder and denser and will continue to rise, subjected to a positive Archimedes' force; similarly, a volume of cold air moving downwards will find itself in hotter, lower density regions of the column and will continue to sink, subjected to a negative Archimedes' force. As a result, an upward heat flux is generated. The process is called convection and the rising and sinking volumes of air are called thermal plumes.

Let us determine the temperature profile corresponding to marginal stability. Consider the displacement of an air parcel from height x_3 to height $x_3 + \mathrm{d}x_3$. Mechanical equilibrium requires that the values of the pressure in and out the parcel remain equal; the final pressure in the parcel will then be $P_L = P(x_3 + \mathrm{d}x_3)$, corresponding to a variation of pressure in the displacement, from Eq. (6.6),

$$\mathrm{d}P_L = -g\rho \mathrm{d}x_3. \tag{6.7}$$

The displacement is supposed to take place on the time scale of the buoyancy forces, which is assumed to be much smaller than the diffusive time scale. This means that during the displacement, the density and the temperature in the parcel evolve along an adiabatic. From Eq. (5.17) and the law of state $P = (k_B/m)\rho T$, we thus get

$$\mathrm{d}P_L = \frac{k_B\rho}{m}\Big(\mathrm{d}T_L + \frac{T_L}{\rho}\mathrm{d}\rho_L\Big) = \frac{kBc_P}{m}\mathrm{d}T_L, \tag{6.8}$$

where $c_P = 1 + c_V$ is the specific heat per molecule at constant pressure. By combining with Eq. (6.7), we find the linear law

$$\mathrm{d}T_L = -\frac{mg}{k_B c_P}\mathrm{d}x_3. \tag{6.9}$$

Equation (5.17) tells us that along an adiabatic the density is inversely proportional to the temperature. Thus, a situation in which T_L grows with x_3 more rapidly than $T(x_3)$ will correspond to unstable conditions. Vice versa, a temperature profile that grows with x_3 more slowly than T_L, will be stable.

We are thus able to conclude that marginal (neutral) stability is realized by an adiabatic temperature profile

$$\frac{\mathrm{d}T}{\mathrm{d}x_3} = \frac{\mathrm{d}T_{adia}}{\mathrm{d}x_3} = -\frac{mg}{k_B c_P}. \tag{6.10}$$

(Note that if the profile is adiabatic, $s =$ constant and any flow in the column is automatically isoentropic.) Unstable stratification corresponds to $\mathrm{d}T/\mathrm{d}x_3 <$

$\mathrm{d}T_{adia}/\mathrm{d}x_3$; stable stratification corresponds to $\mathrm{d}T/\mathrm{d}x_3 > \mathrm{d}T_{adia}/\mathrm{d}x_3$. In the atmosphere, isothermal conditions, $\mathrm{d}T/\mathrm{d}x_3 = 0$ and so-called inversion regimes $\mathrm{d}T/\mathrm{d}x_3 > 0$ are typically considered strongly stable conditions.

6.2 Suggested reading

- L.D. Landau and E.M. Lifshitz, "Fluid mechanics" Vol. 6, Secs. 3 and 4 (Pergamon Press 1987)

7 Compressible flows

We have seen two examples of compressible flows in the production of sound waves and convection; a third trivial mechanism is the presence of a slowly varying force, such as the one exerted by a piston on the gas in a cylinder; a fourth mechanism is provided by the inertia of the flow. Let us focus on this particular mechanism in the case of a gas obeying the law of state Eq. (4.14).

We can estimate the pressure perturbation $\tilde{P}$ generated by the flow, in the absence of external forcing, from the Navier-Stokes equation (4.4). We find

$$\tilde{P} \sim \rho \max(U^2, \nu U/L), \tag{7.1}$$

where U and L are the characteristic space and velocity scales of the flow. By combining Eq. (7.1) with the law of state Eq. (4.14), we then get the relation for the density and the temperature perturbations $\tilde{\rho}$ and $\tilde{T}$:

$$\frac{\tilde{\rho}}{\bar{\rho}} + \frac{\tilde{T}}{\bar{T}} \sim \frac{\tilde{P}}{\bar{P}} \sim \frac{\max(U^2, \nu U/L)}{v_{th}^2} = \mathrm{Ma}^2 \max(1, \mathrm{Re}^{-1}), \tag{7.2}$$

where overbar indicates equilibrium quantities, and where we have introduced the Mach number

$$\mathrm{Ma} = \frac{U}{c_s} \sim \frac{U}{v_{th}}. \tag{7.3}$$

An interesting relation can be established between the Mach number, the Reynolds number and the Knudsen number. From the expression for the kinematic viscosity $\nu \sim \lambda v_{th}$, where λ is the mean free path (see Eqs. (4.9) and (4.17)), we get

$$\mathrm{Re}\,\mathrm{Kn} \sim \mathrm{Ma}. \tag{7.4}$$

For the gas to behave like a simple fluid, we need that $\mathrm{Kn} \ll 1$; the relation $\mathrm{Ma}^2/\mathrm{Re} \sim \mathrm{Kn}^2\mathrm{Re}$ then tells us, from Eq. (7.2), that $\tilde{P}/\bar{P} \sim 1$ only if Re and Ma are both large.

To obtain $\tilde{\rho}/\bar{\rho}$ and $\tilde{T}/\bar{T}$, we exploit the heat transport equation (5.10), which, in a high Re regime, approximates to

$$D_t T + \frac{1}{c_V} T \nabla \cdot \rho \simeq 0 \Rightarrow \frac{\dot{\tilde{T}}}{\bar{T}} \sim \frac{\dot{\tilde{\rho}}}{\bar{\rho}} \Rightarrow \frac{\tilde{\rho}}{\bar{\rho}} \sim \frac{\tilde{T}}{\bar{T}}. \tag{7.5}$$

By combining Eqs. (7.1-7.5), and assuming $\mathrm{Re} \gg 1$, we then get

$$\frac{\tilde{P}}{\bar{P}} \sim \frac{\tilde{\rho}}{\bar{\rho}} \sim \frac{\tilde{T}}{\bar{T}} \sim \mathrm{Ma}^2. \tag{7.6}$$

We reach the result that high Mach number flows are typically compressible. We note that hypersonic flows generate temperature perturbations that may be much higher

than the ambient temperature. This is, of course, of some relevance in hypersonic aircraft design.

As a last point, let us determine the conditions for a compressible flow generation by a moving body. We have seen two examples in the compression of a fluid in a cylinder by a moving piston and the production of sound waves by the membrane of a loudspeaker. Let us determine the conditions for sound generation and study the flow generated by a solid body oscillating with frequency ω. The balance in Eq. (7.1) is replaced in this case by

$$\tilde{P} \sim L\omega\bar{\rho}u \Rightarrow \frac{\tilde{\rho}}{\bar{\rho}} \sim \frac{u}{c_S}\omega L, \tag{7.7}$$

where L is the characteristic size of the body and where we have exploited Eq. (7.5). We see that for the compression contribution in the continuity equation (3.2) to be significant, we need

$$\frac{\tilde{\rho}}{\bar{\rho}} \sim \frac{u}{L\omega} \Rightarrow \frac{\omega L}{c_s} \sim 1, \tag{7.8}$$

which means that sound waves with frequency ω must have a wavelength comparable with L. The compression, and therefore also the sound intensity, is smaller at frequencies $\omega < c_s/L$ (that is why low frequencies require loudspeakers with large woofers).

7.1 The Boussinesq approximation

We want to study convection in a range of scale L such that the variations of equilibrium quantities with height can be considered small,

$$\frac{L\partial_3\bar{\rho}}{\bar{\rho}}, \frac{L\partial_3\bar{T}}{\bar{T}} = O(\epsilon), \qquad \epsilon \ll 1. \tag{7.9}$$

We use the ansatz

$$\frac{\tilde{T}}{\bar{T}} \sim \frac{\tilde{\rho}}{\bar{\rho}} \sim \epsilon, \tag{7.10}$$

and also assume that the plumes have characteristic size $l \ll L$, with

$$\frac{l}{L} \sim \epsilon, \tag{7.11}$$

in such a way that

$$\frac{|\nabla\tilde{\rho}|}{|\partial_3\bar{\rho}|} \sim \frac{|\nabla\tilde{T}|}{|\partial_3\bar{T}|} \sim 1. \tag{7.12}$$

We can estimate the magnitude of the velocity and pressure perturbation directly from the Navier-Stokes equation (4.4). At $O(\epsilon^0)$, of course, we get the hydrostatic balance condition $\partial_3 \bar{P} = -g\bar{\rho}$. To find something more interesting, we must go to $O(\epsilon)$:

$$\bar{\rho} D_t \mathbf{u} + \nabla \tilde{P} = \mu[\nabla^2 \mathbf{u} + (1/3)\nabla(\nabla \cdot \mathbf{u})] - g\tilde{\rho}\mathbf{e}_3. \tag{7.13}$$

In order for convective motions to be established, the buoyancy force $\tilde{\rho} g$ must be sufficiently strong to overcome the viscous force $\mu \nabla^2 u$. This leads to the dominant balance in Eq. (7.13)

$$\bar{\rho}\mathbf{u} \cdot \nabla \mathbf{u} \sim \nabla \tilde{P} \sim -g\tilde{\rho}\mathbf{e}_3 \Rightarrow U^2 \sim lg\epsilon, \ \frac{\tilde{P}}{\bar{P}} \sim \mathrm{Ma}^2 \sim \frac{lg\epsilon}{v_{th}^2}, \tag{7.14}$$

and the condition of neglible viscous forces is just that the Reynolds number $\mathrm{Re} = Ul/\nu \sim l^{3/2}(g\epsilon)^{1/2}/\nu$ is large.

We assume that the Mach number is negligible, which allows us to set, from Eq. (7.14),

$$\tilde{P}/\bar{P} = 0. \tag{7.15}$$

We thus get, from the law of state Eq. (4.14),

$$\frac{\tilde{\rho}}{\bar{\rho}} = -\frac{\tilde{T}}{\bar{T}}. \tag{7.16}$$

Substituting Eq. (7.16) into the continuity equation (3.2), allows us to estimate compression:

$$\nabla \cdot \mathbf{u} = -\Big(\frac{D_t \tilde{\rho}}{\bar{\rho}} + \frac{u_3 \partial_3 \bar{\rho}}{\bar{\rho}}\Big) = \frac{D_t \tilde{T}}{\bar{T}} - \frac{u_3 \partial_3 \bar{\rho}}{\bar{\rho}}, \tag{7.17}$$

where use has been made of Eq. (7.12), and we have kept terms up to $O(\epsilon)$. We can compare compression with the other components of the velocity gradient

$$\frac{\nabla \cdot \mathbf{u}}{||\nabla \mathbf{u}||} \sim \frac{u_3 \partial_3 \bar{\rho}}{\bar{\rho}||\nabla \mathbf{u}||} \sim \frac{l}{L} \sim \epsilon. \tag{7.18}$$

To lowest order in ϵ, the continuity equation then coincides with the incompressibility constraint

$$\nabla \cdot \mathbf{u} = 0. \tag{7.19}$$

By substituting Eq. (7.16) into Eq. (7.13), and taking into account Eq. (7.19), we get the following approximate form of the Navier-Stokes equation

$$\bar{\rho} D_t \mathbf{u} + \nabla \tilde{P} = \mu \nabla^2 \mathbf{u} + \frac{g\bar{\rho}}{\bar{T}} \tilde{T} \mathbf{e}_3. \tag{7.20}$$

Next, we apply the ansatz in Eqs. (7.9-7.11) to the equation for heat transport (5.10). We can verify that the two terms D_tT and $T\nabla\cdot\mathbf{u}$ in Eq. (5.10) are both $O(\epsilon)$. At $O(\epsilon)$, the transport term reads $D_tT = D_t\tilde{T} + u_3\partial_3\bar{T}$. We then substitute Eq. (7.17) into Eq. (5.10) and we get

$$c_P D_t\tilde{T} = \kappa\nabla^2\tilde{T} + \hat{h} + u_3\Big(\frac{\bar{T}}{\bar{\rho}}\partial_3\bar{\rho} - c_V\partial_3\bar{T}\Big), \tag{7.21}$$

where $c_P = 1+c_V$ and $\hat{h}$ contains the contribution from external and viscous heating sources.

Equations (7.19-7.21) constitute the Boussinesq approximation for the continuity equation, the Navier-Stokes equation and the heat transport equation.

The term in brackets in the RHS of Eq. (7.21) acts as a source for temperature fluctuations, with the two terms $\propto \partial_3\bar{\rho}$ and $\propto \partial_3\bar{T}$ giving the effect of compression direct contribution from heat transport. We could linearize Eqs. (7.20) and (7.21). By carrying out a normal mode analysis we would then discover that the sign of the term in brackets in the RHS of Eq. (7.21) determines whether the solutions of the system are oscillating or exponentially growing. In fact, the two regimes in which $(\bar{T}/\bar{\rho})\partial_3\bar{\rho} - c_V\partial_3\bar{T}$ is positive and negative, correspond to unstable and stable stratification, respectively, as discussed in Sec. 6.1.

Equations (7.20) and (7.21) take a somewhat simpler form by expressing ρ and T in terms of the so-called potential temperature

$$\Theta \propto T^{c_V/c_P}\rho^{-1/c_P} \propto TP^{-1/c_P}. \tag{7.22}$$

We verify that $\mathrm{d}\Theta = 0$ along an adiabatic; at a fixed pressure, the potential temperature is proportional to the temperature and thus allows us to identify adiabatics by their temperature at a reference pressure.

From Eq. (7.22) we find

$$\partial_3\bar{\Theta} = -\frac{1}{c_P\bar{T}}\Big(\frac{\bar{T}\partial_3\bar{\rho}}{\bar{\rho}} - c_V\partial_3\bar{T}\Big), \tag{7.23}$$

where the term in brackets in the RHS of the equation equals the term in brackets in the RHS of Eq. (7.21). We also find

$$\tilde{\Theta} = \frac{\bar{\Theta}}{\bar{T}}\tilde{T} - \frac{\bar{\Theta}}{c_P\bar{P}}\tilde{P} \simeq \frac{\bar{\Theta}}{\bar{T}}\tilde{T} \Rightarrow D_t\tilde{\Theta} \simeq \frac{\bar{\Theta}}{\bar{T}}D_t\tilde{T}, \tag{7.24}$$

where use has been made of Eqs. (7.11) and (7.15). We substitute Eqs. (7.23) and (7.24) into Eqs. (7.20) and (7.21), and obtain the following alternative form for the momentum and heat balance equations in the Boussinesq approximation:

$$D_t\mathbf{u} + \frac{1}{\bar{\rho}}\nabla\tilde{P} = \nu\nabla^2\mathbf{u} + \frac{g\bar{\rho}}{\bar{\Theta}}\tilde{\Theta}\mathbf{e}_3, \tag{7.25}$$

$$c_P D_t\tilde{\Theta} = \kappa\nabla^2\tilde{\Theta} + \hat{h} - c_P u_3\partial_3\bar{\Theta}. \tag{7.26}$$

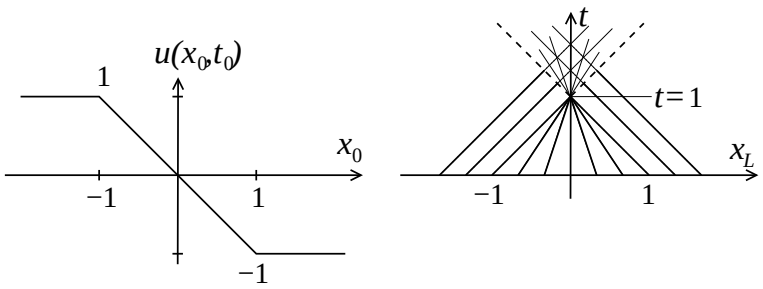

Figure 13: Characteristic lines (right) of the Burgers equation originating from a piecewise linear initial condition for u (left). The solution of the inviscid Burgers equation becomes multivalued in the space-time region above the dashed lines.

7.2 The Burgers equation

The hypersonic limit $\mathrm{Ma} \gg 1$ corresponds to a regime in which the pressure $P \sim \rho v_{th}^2$ is much smaller than the kinetic energy density $(\rho/2)u^2$. The zero-pressure version of the Navier-Stokes is called the Burgers equation, which, for negligible viscosity and in the absence of external forces takes a particularly simple form:

$$D_t \mathbf{u} = 0. \tag{7.27}$$

In a Burgers dynamics, fluid elements move at constant velocity along straight trajectories:

$$\mathbf{u}_L(t|\mathbf{x}_0, t_0) = \mathbf{u}(\mathbf{x}_0, t_0) \Rightarrow \mathbf{x}_L(t|\mathbf{x}_0, t_0) = \mathbf{x}_0 + \mathbf{u}(\mathbf{x}_0, t_0)(t - t_0). \tag{7.28}$$

This allows mapping the solution of the inviscid Burgers equation, which is a partial differential equation, to the solution of the ordinary differential equation $\dot{\mathbf{x}}_L = \mathbf{u}_L$. The approach is common to other first-order partial differential equations, such as e.g. the Hamilton-Jacobi equation, and is called the method of characteristics; the trajectories x_L in the case of the Burgers equation, and (p, q) in the case of the Hamilton-Jacobi equation, are called the characteristic curves.

The graph in $(\mathbf{x}, t)$ of the characteristic curves of the Burgers equation is composed of straight lines, whose orientation is determined by the initial value of $\mathbf{u}$. Depending on the choice of the initial condition $\mathbf{u}(\mathbf{x}_0, 0) = u_L(t|\mathbf{x}_0, 0)$, the characteristic curves may intersect, and the solution of the inviscid Burgers equation may become multivalued. In one dimension, this happens for $u\partial_x u < 1$. The situation is illustrated in Fig. 13: fluid parcels starting from the left with a high velocity, eventually catch back slower fluid parcels starting from the right. The fluid velocity thus becomes multivalued at times $t > 1 + |x_0|$.

The finite-time break-up of the solutions of the inviscid Burgers equations is a consequence of the fact that there are no pressure forces available to prevent fluid parcels from compenetrating each other. This corresponds to a break-up of the fluid

description of the medium. Indeed, the intersecting characteristic curves describe a superposition of fluid jets, which could be interpreted, in a kinetic theory picture, as a non-equilibrium velocity distribution (note that each jet is monochromatic, as the thermal velocity $v_{th} \sim \sqrt{P/\rho} \to 0$ in the regime considered). Now, such a superposition of jets can only survive in a transition region whose size is of the order of the mean free-path λ, where the characteristic curves terminate and the velocity $\mathbf{u}$ is allowed to change.

7.2.1 Viscous Burgers equation

A possibility to account for the presence of transition regions in a Burgers dynamics, is to add a viscous term to Eq. (7.27):

$$D_t u = \nu \partial_x^2 u. \tag{7.29}$$

It is important to note that the viscosity coefficient in Eq. (7.29) has nothing to do with the viscosity in the Navier-Stokes equation: the condition that the velocity differences at scale λ are $\ll v_{th}$ is indeed violated. The choice allows us, however, to explore, in a simple setting the nature of the zero-viscosity limit of fluid mechanics. We are going to see that the limit is singular, in the sense that the solution of the inviscid Burgers equation and of the zero-viscosity limit of the solutions of the viscous Burgers equation is different.

Let us verify this fact and solve Eq. (7.29) with boundary conditions

$$u(\pm\infty, t) = \mp 1, \tag{7.30}$$

and initial condition as in Fig. 13. Let us take $t \gg 1$ and look for stationary solutions to the problem.

Equation (7.29) reads at stationarity,

$$(1/2)\partial_x u_\nu^2 = \nu \partial_x^2 u_\nu \Rightarrow \nu \partial_x u_\nu - u_\nu^2/2 = \pm a^2, \tag{7.31}$$

where a is a constant. Let us solve Eq. (7.31) in the case a^2 come with the minus sign and verify that the choice allows us to enforce the boundary conditions in Eq. (7.30) and Fig. 13. Define $u_\nu = a\hat{u}$ and indicate with prime derivative with respect to x. We get

$$\frac{\hat{u}'}{\hat{u}^2 - 1} \equiv (\arctan \hat{u})' = -\frac{a}{2\nu} \Rightarrow \hat{u} = \tanh\left(b - \frac{ax}{2\nu}\right), \tag{7.32}$$

where b is another constant. The boundary condition (7.30) imposes $a = 1$ and the initial condition in Fig. 13 requires the solution to be antisymmetric, hence $b = 0$. We thus obtain the result

$$u_\nu(x) = -\tanh\left(\frac{x}{2\nu}\right). \tag{7.33}$$

The limit $\nu \to 0$ in Eq. (7.33) corresponds to a step-function solution

$$u(x) = -1 + 2\theta(x), \tag{7.34}$$

which does not coincide with the solution of Eq. (7.27) with the same boundary conditions. We can adapt the description to the case in which $u(-\infty) \neq -u(+\infty)$ by a mere change of reference frame. In general we get

$$u(x) = u(-\infty) + 2U\theta(x - x_0 - Ut), \qquad U = \frac{u(+\infty) - u(-\infty)}{2}, \tag{7.35}$$

where x_0 is the initial position of the discontinuity.

Equation (7.35) describes a situation in which the mass of the fluid is transported to the transition region, leading to the formation of a singularity in the mass distribution. An initially uniform mass distribution thus evolves into an ensemble of spikes, interspersed by voids, whose position and translation velocity is determined by the initial fluid velocity profile. It is easy to be convinced that in two and three dimensions, the spikes are replaced by singular mass distributions setting the boundary of two and three-dimensional voids.

The Burgers dynamics does not explain why the mass should stick at the singular boundary of such voids instead of diffusing or bouncing back. In a cosmological setting, models based on a Burgers equation approach have been used to describe the formation of large-scale structures such as galaxies and clusters, in which case an obvious adhesion mechanism is gravity. In a gas dynamics context, no such mechanism exists and Eqs. (7.34) and (7.35) cannot describe a stationary condition.

Stationarity requires that there is no accumulation of mass in the discontinuity. The the mass current ρu must therefore satisfy

$$\rho_- u_- = \rho_+ u+, \tag{7.36}$$

where u is measured in the reference frame of the discontinuity and $\pm$ indicate values of ρ and u at the two sides of it. Similar continuity conditions must be imposed on the momentum and energy flux. Such a stationary discontinuity is called a shock wave.

The main difference between Eqs. (7.34) and (7.36) is that in the latter, matter flows across the discontinuity rather into it. We can thus envision a shock wave as the result of a low-density high-velocity gas jet impinging on gas with a higher density. It is possible to show by solving Eq. (7.36) and the continuity equations for momentum and energy at the shock, that in the high density region the pressure is higher than in the jet, and that the Mach number in the reference frame of the shock is < 1. On the other hand, the Mach number of the jet measured in the reference frame of the shock is > 1. Thus, contrary to the picture provided by the Burgers equation, in which $\mathrm{Ma} > 1$ everywhere, shock waves in compressible flows separate supersonic from subsonic regions.

7.2.2 The method of characteristics

A first order PDE for a field $u = u(\mathbf{z})$ can be written in the most general form as

$$F(\mathbf{z}, u, \boldsymbol{\pi}) = 0, \qquad \pi_i = \partial_{z_i} u. \tag{7.37}$$

In the case of the 1D Burgers equation,

$$F = \pi_1 + u\pi_2 = 0, \qquad z_1 = t, \quad z_2 = x. \tag{7.38}$$

In the case of the Hamilton-Jacobi equation $\dot{S} + H(\partial_q S, q, t)$, $u \equiv S$ is the action and Eq. (7.37) takes the form

$$F = \pi_1 + H(\pi_2, z_2, z_1) = 0, \qquad z_1 = t, \quad z_2 = q. \tag{7.39}$$

The method could be generalized to the case $\mathbf{F}$ is a vector, and $\mathbf{u}$ is a vector field.

The solution of Eq. (7.37) by the methods of characteristic is obtained by writing $u = u(z_i)$ in the parametric form $u = u(z_i(s|z_0))$, where the $z_i = z_i(s|z_0)$ are the characteristic curves of the equation. Suppose we have such a solution. By differentiating Eq. (7.28) along a characteristic curve, we would then obtain

$$\begin{aligned} 0 = \dot{F} &= \dot{z}_i \partial_{z_i} F + \dot{z}_i (\partial_{z_i} u) \partial_u F + \dot{\pi}_i \partial_{\pi_i} F \\ &= \dot{z}_i (\partial_{z_i} F + \pi_i \partial_u F) + \dot{\pi}_i \partial_{\pi_i} F, \end{aligned} \tag{7.40}$$

where dot indicates total derivative with respect to s. We solve Eq. (7.40) through the ansatz

$$\dot{z}_i = \lambda \partial_{\pi_i} F, \tag{7.41}$$

where λ is an arbitrary parameter (in general a function of $\mathbf{z}$ and s). By substituting Eq. (7.41) into Eq. (7.40) we get

$$\dot{\pi}_i = -\lambda(\partial_{z_i} F + \pi_i \partial_u F), \tag{7.42}$$

and by substituting Eq. (7.41) into the relation $\dot{u} = \dot{z}_i \partial_{z_i} u = \dot{z}_i \pi_i$,

$$\dot{u} = \lambda \pi_i \partial_{\pi_i} F. \tag{7.43}$$

The characteristic curves are obtained by solving the system formed by Eqs. (7.41) and (7.43):

$$\dot{z}_i = \lambda \partial_{\pi_i} F, \qquad \dot{u} = \lambda \pi_i \partial_{\pi_i} F, \tag{7.44}$$

in which different choices of λ lead to different parameterizations of the curves.

We can apply the method to the solution of the Hamilton-Jacobi equation. We verify that the choice $\lambda = 1$, $z_1 = t = s$ gives us back Hamilton's equations. From the first component of Eq. (7.41) we get the identity $\dot{z}_1 = \partial_{\pi_1} F = 1$, and the second component gives us

$$\dot{z}_2 \equiv \dot{q} = \partial_{\pi_2} F = \partial_p H \tag{7.45}$$

that is Hamilton's equation for q. Since F does not depend explicitly in S, Eq. (7.42) becomes $\dot{\pi}_i = \partial_{z_1} F$. The first component of the equation yields the identity $\ddot{S} = -\dot{H}$, and the second component gives us Hamilton's equation for p:

$$\dot{\pi}_2 \equiv \dot{p} = -\partial_{z_2} F = -\partial_q H. \tag{7.46}$$

7.3 Suggested reading

- L.D. Landau and E.M. Lifshitz, "Fluid mechanics" Vol. 6, Secs. 10 and 82-84 (Pergamon Press 1987)

8 Ideal and viscous flows

We say that a fluid is ideal if its viscosity is equal to zero. Unfortunately, the zero viscosity limit of the Navier-Stokes equation (4.4) is singular, which means that the zero viscosity limit of its solution does not coincide in general with the solution of the Euler's equation (5.27). We have seen an example of such behavior in Sec. 7.2, when comparing the solutions of the inviscid and viscous Burgers equation. We shall see that a crucial role in the dynamics of a viscous fluid is played by vorticity. Indeed, one of the mechanisms of vorticity generation is the interaction of a viscous fluid with a solid object. The mechanism is easy to understand.

Consider a portion of the surface of the solid, sufficiently small to be approximated by its tangent plane, which we take to be the x_1x_2 plane. At a sufficiently small distance, the flow in the reference frame of the body is almost parallel to the body's surface and is a linear function of x_3. Taking the flow locally along x_1, $\mathbf{u} = (\alpha x_3, 0, 0)$, which corresponds to values of the viscous stress and the viscosity $\sigma_{13} = \alpha\mu$ and $\boldsymbol{\omega} = (0, \alpha, 0)$.

What happens in high Reynolds number flows is that the velocity gradient tends to be concentrated in a boundary layer whose thickness decreases with the viscosity. In the case of slowly varying flows, the boundary layer thickness l can be estimated from the Navier-Stokes equation (4.4), as the distance from the body at which inertia and viscous dissipation become of the same order. We get $l \sim \nu/U$, where U is the velocity scale of the flow relative to the body. The intensity of the gradient, on the other hand, can be estimated as $\alpha \sim U/\delta \sim U^2/\nu$. For small ν, the boundary layer becomes very thin, but the viscous stress becomes large in proportion. Furthermore, if the flow becomes turbulent, vorticity is transported away from the obstacle and may end up filling a significant portion of the fluid, in the form of intertwined very thin vortex filaments and surfaces. Therefore, a zero viscosity limit does not necessarily correspond to a zero viscous dissipation limit. Notwithstanding, if turbulence remains confined to a limited portion of the fluid, the flow could be treated as ideal away from solid obstacles and the turbulence they generate. An example of such an approach is provided by the discussion of the Magnus effect in Sec. 5.5.

The opposite limit of a strongly viscous flow corresponds to a small Re number regime, in which the advection term in the Navier-Stokes equation can be disregarded. We have seen in the the discussion leading to Eq. (7.6)), that the $\mathrm{Re} = 0$ limit of the Navier-Stokes equation corresponds to an incompressible regime. The limit is non-singular and is realized by the Stokes equation

$$\rho\partial_t\mathbf{u} + \nabla P = \mu\nabla^2\mathbf{u} + \mathbf{f}^{ext}, \qquad \nabla\cdot\mathbf{u} = 0. \tag{8.1}$$

Note that $\mathbf{f}^{ext}$ may have a compressible component, $\nabla\cdot\mathbf{f}^{ext} \neq 0$. However, unless the variation of time of $\mathbf{f}^{ext}$ is so fast to generate sound waves, we can reabsorb the compressible part of $\mathbf{f}^{ext}$ in a hydrostatic component of the pressure, P^{hs}, obeying $\nabla^2 P^{hs} = \nabla\cdot\mathbf{f}^{ext}$. Once this component is subtracted, we verify that the pressure

obeys Laplace's equation

$$\nabla^2 P = 0. \tag{8.2}$$

By taking the curl of Eq. (8.1) we obtain the vorticity equation

$$\rho \partial_t \boldsymbol{\omega} = \mu \nabla^2 \boldsymbol{\omega} + \nabla \times \mathbf{f}^{ext}. \tag{8.3}$$

We note that low Reynolds number flows are characterized by space and velocity scales that are very small compared with the experience of everyday life; for instance, a flow in a pipe, with a velocity at the center of the pipe $U \sim 1\,\mathrm{cm/s}$, would require, to satisfy $\mathrm{Re} < 1$, $L < 0.1\,\mathrm{mm}$.

8.1 Potential flows

The velocity field of a vorticity-free flow can be written as the gradient of a scalar potential

$$\mathbf{u} = \nabla \Phi. \tag{8.4}$$

We speak in this case of a potential flow. If the fluid is barotropic, and the external force can itself be derived from a potential, $\mathbf{f}^{ext}/\rho = -\nabla \Psi$, the Navier-Stokes equation can be converted into an equation for the potential

$$\partial_t \Phi + \frac{1}{2}|\nabla \Phi|^2 + w + \Psi - \frac{4}{3}\nu \nabla^2 \Phi = \text{constant}, \tag{8.5}$$

where w is the enthalpy per unit mass of the fluid, and where we have exploited the relation

$$\begin{aligned} \mathbf{u} \cdot \nabla u_j &= (\partial_i \Phi)\partial_j \partial_i \Phi = \partial_j[(\partial_i \Phi)\partial_i \Phi] - (\partial_j \partial_i \Phi)\partial_i \Phi \\ &= \partial_j[(\partial_i \Phi)\partial_i \Phi] - \frac{1}{2}\partial_j[(\partial_i \Phi)\partial_i \Phi] = \frac{1}{2}\partial_j |\nabla \Phi|^2. \end{aligned} \tag{8.6}$$

We note that the constant in Eq. (8.5) may still depend on time; such time dependence would produce a contribution to Φ, which is time-dependent but constant in space, and thus does not modify $\mathbf{u}$.

Equation (8.6) tells us that in barotropic conditions, a vorticity-free initial condition produces zero curl terms in the Navier-Stokes equation. A flow which has zero vorticity initially, will thus remain vorticity-free at later times.

Equation (8.5) takes a particularly simple form in the incompressible case

$$\partial_t \Phi + \frac{1}{2}|\nabla \Phi|^2 + \frac{P}{\rho} + \Psi = \text{constant}, \qquad \nabla^2 \Phi = 0, \tag{8.7}$$

in which the viscous terms disappear, and the dynamics becomes identical to that of an ideal fluid (in this case, the flow contains only strain). We note that in the case

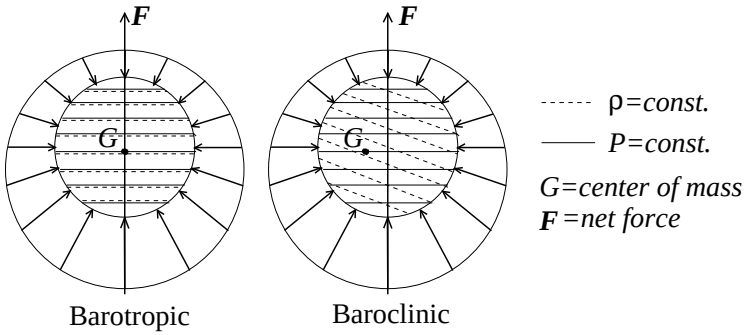

Figure 14: Mechanism of vorticity generation in baroclinic conditions (from *Fluid Mechanics* by P. Kundu).

of a time-independent ideal flow, Eq. (8.5) takes a form reminiscent of Bernoulli's equation

$$\frac{1}{2}|\nabla\Phi|^2 + w + \Psi = \text{constant}, \tag{8.8}$$

the only difference being that in the case of Bernoulli's equation the sum $u^2/2+w+\Psi$, is constant along flow lines, while in the case of Eq. (8.8) the sum is constant in the whole flow domain.

To solve Eq. (8.5), we must impose boundary conditions on the potential Φ; we require that the fluid cannot penetrate solid objects (impermeability boundary conditions), which leads to Neumann boundary conditions at the body surface s

$$\mathbf{u}_\perp^{solid} = \mathbf{u}_\perp^s = \nabla_\perp \Phi^s, \tag{8.9}$$

where $\mathbf{e}_\perp$ is the local normal to the solid surface. We note that no boundary conditions are imposed on the tangential component of the velocity; however, we know that viscosity generates tangential stress at the solid surface, which forces the tangential components of $\mathbf{u}$ and $\mathbf{u}^{solid}$ at the solid surface to be equal:

$$\mathbf{u}_\parallel^{solid} = \mathbf{u}_\parallel^s. \tag{8.10}$$

In general $\mathbf{u}_\parallel^{solid} \neq \nabla_\parallel \Phi$, and the difference $\mathbf{u}_\parallel^{solid} - \nabla_\parallel \Phi$ acts as a source of vorticity.

Another mechanism for vorticity production is the presence of baroclinic conditions, as illustrated in Fig. 14. The baroclinic case in the figure corresponds to a situation in which the temperature is higher to the right (the fluid element may represent the left lobe in the vertical section of a rising mushroom cloud). The center of mass of the fluid element shifts to the left, which causes the gravitational force to generate a counterclockwise torque on the fluid element.

8.2 Fluid inertia

We want to study the dynamics of a solid body in an infinite fluid, for frequencies and velocities small enough to be able to consider the fluid incompressible. We focus on the conservative component of the dynamics and make the assumption that the flow is potential.

Indicate with $\mathbf{U}$ the velocity of the body and with $\mathbf{u}(\mathbf{x}, t)$ the velocity perturbation generated in the fluid. We consider for simplicity the case of a sphere of radius R moving along the axis x_1. Indicate with $\hat{\mathbf{u}} = \nabla\hat{\Phi}$ the fluid velocity perturbation in the reference frame of the moving sphere. If $\mathbf{U}$ were constant,

$$\hat{\mathbf{u}}(\mathbf{x}, t) = \mathbf{u}(\mathbf{x} + \mathbf{U}t, t). \tag{8.11}$$

We obtain the field $\hat{\mathbf{u}}$ as the solution to the boundary value problem

$$\nabla^2\hat{\Phi} = 0, \qquad \mathbf{x} \cdot (\mathbf{U} + \hat{\mathbf{u}})_A = 0, \tag{8.12}$$

where A is the sphere's surface and we have put the origin of the axes at the center of the sphere.

The potential $\hat{\Phi}$ has the same structure of the electrostatic potential of a multipole, which, if the volume of fluid is infinite, reads

$$\Phi(\mathbf{x}) = -\frac{M^{(0)}}{x} - \frac{\mathbf{M}^{(1)} \cdot \mathbf{x}}{x^3} - \frac{\mathbf{M}^{(2)} : \mathbf{xx}}{x^5} + \dots \tag{8.13}$$

We know from incompressibility, that the point charge contribution to $\hat{\mathbf{u}}$, $\hat{\mathbf{u}}^{(0)} = M^{(0)}\mathbf{x}/x^3$, must vanish. We verify that to enforce the boundary conditions in Eq. (8.12), it is sufficient to keep the dipole contribution:

$$\hat{\mathbf{u}} = \hat{\mathbf{u}}^{(1)} = \frac{3(\mathbf{M}^{(1)} \cdot \mathbf{x})\mathbf{x} - \mathbf{M}^{(1)}x^2}{x^5}. \tag{8.14}$$

In fact, we know from symmetry, that $\mathbf{M}^{(1)}$ is directed along x_1; we can thus write

$$\mathbf{x} \cdot (\mathbf{U} + \hat{\mathbf{u}})_A = 2R^{-2}M^{(1)}z + URz = 0, \tag{8.15}$$

where $z = x_1/x$. By exploiting Eq. (8.14) we get

$$\hat{\mathbf{u}} = \frac{[\mathbf{U}x^2 - 3(\mathbf{U} \cdot \mathbf{x})\mathbf{x}]R^3}{2x^5}. \tag{8.16}$$

From Eq. (8.16), we can calculate the kinetic energy content of the velocity perturbation generated in the fluid by the moving sphere:

$$K = \frac{\rho R^6 U^2}{8} \int_R^{+\infty} \frac{\mathrm{d}x}{x^4} \int_{-1}^{1} \mathrm{d}z\,(3z^2 + 1) = \frac{\rho R^3 U^2}{6}. \tag{8.17}$$

Equation (8.17) tells us that the work to put in motion a body in an ideal fluid contains a component associated with the induced fluid motion, which has the same

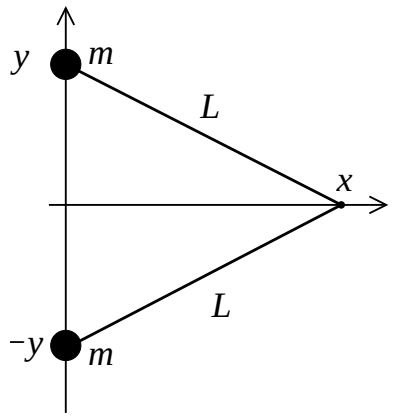

Figure 15: Mechanical analog of the incompressible fluid. The two beads, which represent the fluid, are free to slide vertically on the y axis and are connected to the hinge in x (the solid body) by two rigid sticks of length L (the pressure and impermeability constraints).

effect as a renormalization of the mass of the body; the mass correction, called added mass depends on the body shape and the fluid density. In the case of a sphere, from Eq. (8.17)

$$\delta M = \frac{\rho R^3}{3}. \tag{8.18}$$

From Eq. (8.17), we can define the linear momentum of the flow perturbation

$$\delta \mathbf{P} = \frac{\partial K}{\partial \mathbf{U}} = \delta M \mathbf{U}. \tag{8.19}$$

Note that $\delta\mathbf{P}$ cannot be expressed as an integral over the linear momenta of the fluid elements, as K receives contributions from momenta both along $\delta\mathbf{P}$ and perpendicular to it. In fact, the integral $\rho \int \mathrm{d}^3x \hat{\mathbf{u}}$ does not even converge. A simple mechanical analog, showing a similar mismatch between total momentum and sum of the momenta of the parts, is shown in Fig. 15. The Lagrangian of the system is

$$L(x, \dot{x}) = m\dot{y}^2 = \frac{mx^2\dot{x}^2}{L^2 - x^2} \tag{8.20}$$

and the momentum conjugate to x is

$$p = \frac{\partial L}{\partial \dot{x}} = \frac{2mx^2\dot{x}}{L^2 - x^2}, \tag{8.21}$$

while the sum of the momenta of the two beads, $m\dot{y}$ and $-m\dot{y}$, is by construction equal to zero.

We note that if the velocity $\mathbf{U}$ of the solid body is constant, the total linear momentum $\mathbf{P} = (M + \delta M)\mathbf{U}$ of the system, and the fluid is conserved. We thus reach the remarkable conclusion (d'Alambert's paradox) that no force is required to keep a body in motion in an inviscid infinite fluid. Note that the condition that the fluid is infinite cannot be relaxed, as momentum could flow out of a finite domain without the need for dissipation. A trivial mechanism is the interaction with a moving solid boundary. Another mechanism, in the case of an underwater body, is momentum transport through the generation of gravity waves—an effect known as wave drag.

To accelerate or slow down a body in an infinite inviscid fluid, we still need to impose a force $\mathbf{F} = (M + \delta M)\dot{\mathbf{U}}$. We can use this information to determine the law of motion for a solid body immersed in an accelerating fluid; suppose that the only force on the body is the Archimedes' push from the acceleration of the fluid,

$$V\rho D_t \mathbf{U}_f \equiv V\rho(\partial_t + \mathbf{U}\cdot\nabla)\mathbf{U}_f, \tag{8.22}$$

where V is the volume of the body, $\mathbf{U}_f$ is the fluid velocity and $D_t\mathbf{U}_f$ is the change of fluid velocity experienced by the moving body. The Archimedes forces generates a variation in the momentum of the body $M\mathbf{U}$ and in the momentuom of the perturbation in the fluid $\delta M(\mathbf{U} - \mathbf{U}_f)$. The result is

$$(M + \delta M)\dot{\mathbf{U}} = (V\rho + \delta M)D_t\mathbf{U}_f. \tag{8.23}$$

Thus, the body whose density is larger than the fluid's; vice versa if if the body's density is smaller than the fluid's.

8.3 Gravity waves

Gravity waves are an example of potential flow. We focus on the case of small amplitude gravity waves in deep water; we verify that for reasonable values of the wavelength and of the wave amplitude, viscous stresses are negligible.

Let us choose our reference system with x_1 along the propagation's direction of the wave, with x_3 pointing upwards and the origin of the axes at the unperturbed water surface; we look for solutions in the form

$$\Phi(\mathbf{x}, t) = \Phi_0(x_3)\exp[\mathrm{i}(kx_1 - \omega t)]. \tag{8.24}$$

Incompressibility guarantees that the velocity potential obeys Laplace's equation $\nabla^2\Phi = 0$, which takes the form in the case of the wave solution in Eq. (8.24),

$$(\partial_3^2 - k^2)\Phi_0 = 0 \Rightarrow \Phi_- \mathrm{e}^{-kx_3} + \Phi_+ \mathrm{e}^{kx_3}. \tag{8.25}$$

The term $\Phi_-\mathrm{e}^{-kx_3}$ grows exponentially with the depth and is absent in the case of infinitely deep water.

To obtain a dispersion relation, we require that the fluid pressure at the perturbed water surface equals the atmospheric pressure; this implies

$$\partial_t P_L(t|\mathbf{x},0) = 0, \tag{8.26}$$

where $P_L(t|\mathbf{x},0)$ is the pressure at the position of the fluid element which at time $t = 0$ was at the unperturbed water surface at position $\mathbf{x} \equiv (x_1, x_2, 0)$. To obtain $P_L(t|\mathbf{x},0)$, we first determine $P(\mathbf{x},t)$ from Eq. (8.7). We see that the equation can be linearized provided $k\Phi^2 \ll \omega\Phi$; the meaning of such conditions becomes more transparent if expressed in terms of the wave height A of the wave, which we can put in terms of the velocity potential at the water surface through the relation $\omega A = k\Phi_0(0)$. The condition for small amplitude waves thus becomes

$$kA \ll 1, \tag{8.27}$$

which means that the wavelength must be much longer than the wave amplitude; the linearized version of Eq. (8.7) reads

$$P/\rho = -\partial_t\Phi + gx_3 + \text{constant}. \tag{8.28}$$

We similarly linearize P_L:

$$\begin{aligned} P_L(t|\mathbf{x},0) \equiv P(\mathbf{x}_L(t|\mathbf{x},0),t) &= \rho[gx_{3,L}(t|\mathbf{x},0) - \partial_t\Phi(\mathbf{x}_L(t|\mathbf{x},0),t)] \\ &\simeq \rho[gx_{3,L}(t|\mathbf{x},0) - \partial_t\Phi(\mathbf{x},t)]. \end{aligned} \tag{8.29}$$

By substituting Eq. (8.29) into Eq. (8.26) we then get

$$0 = [g\partial_3 - \partial_t^2]\Phi = 0, \tag{8.30}$$

where we have exploited

$$\dot{x}_{3,L}(t|\mathbf{x},0) = u_{3,L}(t|\mathbf{x},0) \simeq u_3(\mathbf{x},t), \tag{8.31}$$

and use has been made again of Eq. (8.27). We substitute Eqs. (8.24) and (8.25) into Eq. (8.30) and we obtain the dispersion relation

$$\omega^2 = kg. \tag{8.32}$$

From Eq. (8.32), we find for the phase velocity of the wave

$$c_w = g/\omega^2. \tag{8.33}$$

Of course, the form of the dispersion relation could have been guessed from dimensional arguments, except for a dimensionless constant $K = c_w\omega^2/g$, whose value is fixed by the present analysis to 1.

Gravity waves in nature do not always have a small amplitude; it is then of some interest to evaluate the nonlinear corrections to the wave dynamics; we are going to see that nonlinearities generate a transport component in the motion of the fluid.

Let us study the trajectory of a fluid element at the water surface. Such fluid a element will move with velocity $\dot{\mathbf{x}}_L(t|\mathbf{x}) = \mathbf{u}_L(t|\mathbf{x})$. To lowest order in the parameter kA, we can approximate

$$\mathbf{x}_L \simeq \mathbf{x} - A \begin{pmatrix} \cos(\alpha_0 + kx_1 - \omega t) \\ \sin(\alpha_0 + kx_1 - \omega t) \end{pmatrix}, \tag{8.34}$$

where $A = k|\Phi_0(0)|/\omega$ and α_0 is the initial phase of Φ_0. The fluid element moves along a circular trajectory.

Let us evaluate the next order in the expansion

$$\begin{aligned} u^{(2)}_{L,1} &= (\mathbf{x}_L(t|\mathbf{x}) - \mathbf{x}) \cdot \nabla u_1(\mathbf{x}, t) \\ &= \frac{A}{\omega}(\mathbf{x}_L(t|\mathbf{x}) - \mathbf{x}) \cdot \nabla [\mathrm{e}^{kx_3} \sin(\alpha_0 + kx_1 - \omega t)] \end{aligned}$$

and similar expressions for the other components of $\mathbf{u}_L$. We find from Eq. (8.34), at the water surface,

$$u^{(2)}_{L,1} = \frac{kA^2}{\omega}[\sin^2(\alpha_0 + kx_1 - \omega t) + \cos^2(\alpha_0 + kx_1 - \omega t)] = (kA)^2 c_w. \tag{8.35}$$

We see that the fluid motion at the water surface has an $O((kA)^2)$ drift component called the Stokes drift, which can generate transport in the direction of the wave.

8.3.1 Viscous corrections

Treating the velocity field in a gravity wave as a potential flow only required to impose, through Eq. (8.26), continuity of the normal stress at the water surface; this replaces the impermeability condition Eq. (8.9) on the surface of a solid obstacle. Finite viscosity requires us to impose continuity of the tangential stress, which replaces the no-slip boundary condition on the surface of a solid obstacle. We are going to verify that in the case of gravity wave, the effect of viscosity is to generate a boundary layer of negligible thickness, whose effect on the wave dynamics can, in most circumstances, be disregarded.

Since $\mu_{air} \sim 0.015\mu_{water}$, the tangential stress at the water surface can be taken to be zero. Continuity of the tangential stress then implies

$$\partial_3 u_1 = \partial_3(u_1^{vort} + \partial_1 \Phi) = 0, \tag{8.36}$$

which leads to the estimate for the vorticity at the water surface

$$\hat{\omega} \simeq -\partial_3 \partial_1 \Phi \tag{8.37}$$

(we put a hat on $\hat{\omega}$ to distinguish the vorticity from the frequency ω). We can obtain an equation for the vorticity by taking the curl of the Navier-Stokes equation. In

the case of linear waves, the advection term can be disregarded, and we recover Eq. (8.3), which, in the absence of external forcing, becomes a diffusion equation:

$$\partial_t \hat{\boldsymbol{\omega}} = \nu \nabla^2 \hat{\boldsymbol{\omega}}. \tag{8.38}$$

The viscous boundary layer at the water surface has therefore thickness

$$l \sim \sqrt{\nu/\omega}, \tag{8.39}$$

which, frequencies of the order of 1 Hz or smaller, is well below the millimeter scale.

We can estimate the damping rate Γ of the wave as the ratio of the dissipation per unit surface

$$\dot{E} \sim -\mu \int \mathrm{d}x_3 \hat{\omega}^2 \sim \mu l |\Phi k^2|^2 \tag{8.40}$$

and the energy per unit surface of the wave

$$E \sim \rho \int \mathrm{d}x_3 |\nabla \Phi|^2 \sim \rho |\Phi|^2 k, \tag{8.41}$$

where use has been made of Eq. (8.25). We find

$$\frac{\Gamma}{\omega} = \frac{\dot{E}}{\omega E} \sim \frac{\nu l k^3}{\omega} \sim \frac{\nu^{3/2} \omega^{9/2}}{g^3}, \tag{8.42}$$

where use has been made of Eq. (8.33). In order for the ratio Γ/ω to become $O(1)$, it would be necessary to consider very small wavelengths, at the millimeter scale, in which case surface tension becomes significant and gravity wave are replaced by capillary waves.

8.4 Viscous flows

We study viscous flows in a so-called creeping flow regime, characterized by boundary conditions and the external forces changing in time on a time scale much slower than the viscous timescale $\tau = L^2/\nu$. As usual, L is the characteristic scale of the flow. For simplicity, we neglect external forces; the Stokes equation (8.1) takes, in this case, the simple form

$$\nabla P = \mu \nabla^2 \mathbf{u}, \qquad nabla \cdot \mathbf{u} = 0. \tag{8.43}$$

In creeping flow conditions, the fluid velocity $\mathbf{u}(\mathbf{x}, t)$ is determined instantaneously by the boundary conditions of the flow.

Except for very simple geometries, solving Eqs. (8.1) and (8.43) is laborious. Dimensional reasoning though allows one to obtain some estimates. For instance, we get for the drag force on a body of size L moving with velocity U in the fluid:

$$F \sim L^3 \mu \nabla^2 \mathbf{u} \sim \mu L U. \tag{8.44}$$

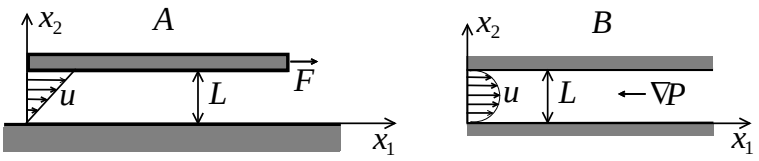

Figure 16: Sketch of Couette flow (A) and channel flow (B).

An exact solution of Eq. (8.43) is possible in the case of the Couette flow, which is the flow between two flat surfaces sliding at constant relative speed U. The geometry of the system is shown in Fig. 16a; we can evaluate the force that is required to keep the system in motion. Let us assume the width of the gap is much smaller than the gap's horizontal extension. This allows us to disregard border effects and to write $\mathbf{u} = (u_1(x_2), 0, 0)$. Since the velocity U of the body is constant, the force F exactly balances the viscous and pressure forces in the fluid. On the other hand, since the fluid does not accelerate, we must have $-\partial_1 P + \mu\partial_2 u = 0$, and if no pressure forces are imposed on the fluid, we can set

$$\partial_2 u = 0. \tag{8.45}$$

We can then impose no-slip conditions (Eq. (8.10)) on the solid surfaces bounding the gap, and we get

$$u(x_2) = Ux_2/L. \tag{8.46}$$

From here, we obtain the expression for the drag force

$$F = \mu AU/L, \tag{8.47}$$

where A is the area of the body.

Another example of a flow for which a simple description is possible, is the channel flow in Fig. 16b. In this case we have a pressure difference ΔP at the two ends of the interstice between two flat solid objects; again, the width of the gap is supposed small compared with its horizontal extension, which implies $\mathbf{u} = (u_1(x_2), 0, 0)$. The condition that the flow is stationary implies

$$\mu\partial_2^2 u = \partial_1 P = \Delta P/X. \tag{8.48}$$

By imposing no-slip conditions on the surfaces at $x_2 = 0$ and $x_2 = L$, we find the parabolic flow profile

$$u(x_2) = \frac{\Delta P}{2\mu X}(L - x_2)x_2. \tag{8.49}$$

The same calculation can be carried out in the case of a flow in a cylindrical pipe (Poiseuille flow), in which case it is possible to show that

$$u(r) = \frac{\Delta P}{4\mu X}(R^2 - r^2), \tag{8.50}$$

where R is the pipe's radius and r is the radial coordinate.

8.5 Suggested reading

- L.D. Landau and E.M. Lifshitz, "Fluid mechanics" Vol. 6, Secs. 9, 11 and 12. (Pergamon Press 1987)
- P. Kundu, "Fluid Mechanics", Secs. 5.1-3 (Ac. Press 2015)

9 Vorticity dynamics

We can obtain an evolution equation for the vorticity $\boldsymbol{\omega} = \nabla \times \mathbf{u}$ by taking the curl of the Navier-Stokes equation (4.4) and exploiting the identity from vector analysis $\nabla u^2/2 = \mathbf{u} \times (\nabla \times \mathbf{u}) + \mathbf{u} \cdot \nabla \mathbf{u}$. The result is

$$D_t \boldsymbol{\omega} - \boldsymbol{\omega} \cdot \nabla \mathbf{u} \equiv (\partial_t + \mathcal{L}_{\mathbf{u}})\boldsymbol{\omega} = -\nabla \times \frac{\nabla P}{\rho} + \nu \nabla^2 \boldsymbol{\omega} + \nabla \times (\mathbf{f}^{ext}/\rho), \tag{9.1}$$

where $\mathcal{L}_{\mathbf{u}}\boldsymbol{\omega}$ is the Lie derivative defined in Eq. (2.17). We see that if the three conditions that viscosity is negligible, the fluid is barotropic and that the external force per unit mass is curl-free are all satisfied, vorticity will behave as a frozen vector field.

This remarkable property has a geometrical origin, which is best understood by looking at the behavior of the flow lines of the vorticity field (the vortex lines). We note that since $\boldsymbol{\omega}$ is by construction divergence-free, the vortex lines must either close on themselves or terminate at the boundaries of the fluid.

We can define the vortex tube generated by a certain closed contour Γ, as the set of the vortex lines girded by Γ (see Fig. 17). The vorticity flux through any surface A bounded by Γ has the same value

$$\varphi_\Gamma = \int_A \mathrm{d}\mathbf{A} \cdot \boldsymbol{\omega} = \int_\Gamma \mathrm{d}\mathbf{l} \cdot \mathbf{u}, \tag{9.2}$$

which defines the strength of the vortex tube.

We can verify that φ_Γ does not depend on the choice of the countour Γ. Consider the portion V of the vortex tube in Fig. 17. From the fact that the vorticity is a zero-divergence field, we have in fact

$$0 = \int_V \mathrm{d}V \, \nabla \cdot \boldsymbol{\omega} = \int_{\partial V} \mathrm{d}\mathbf{A} \cdot \boldsymbol{\omega} = \int_{A'} \mathrm{d}\mathbf{A}' \cdot \boldsymbol{\omega} - \int_A \mathrm{d}\mathbf{A} \cdot \boldsymbol{\omega} = \varphi_{\Gamma'} - \varphi_\Gamma, \tag{9.3}$$

where we have exploited the fact that $\boldsymbol{\omega}$ is by construction parallel to the surface of the vortex tube.

9.1 Kelvin's theorem

If the flow is time-dependent, the geometry of vortex lines and vortex tubes will not remain constant. However, if the flow is inviscid and barotropic, and the external force can be derived from a potential, $\mathbf{f}^{ext}/\rho = -\nabla\Psi$, the strength φ_Γ of vortex tubes is conserved. This is equivalent to the statement, which is the content of Kelvin's theorem, that if the above conditions are satisfied, the velocity circulation along a contour $\Gamma_L(t)$ moving with the fluid is a constant of the motion:

$$\varphi_{\Gamma_L} = \int_{\Gamma_L} \mathrm{d}\mathbf{l} \cdot \mathbf{u} = \text{constant}. \tag{9.4}$$

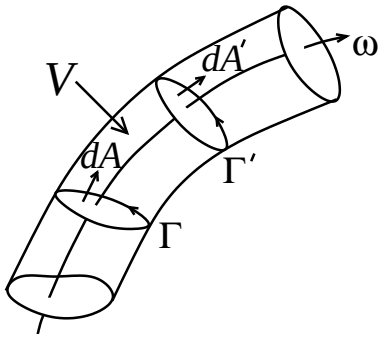

Figure 17: Representation of a vortex tube.

Let us prove the result. The circulation of $\mathbf{u}$ along a path Γ, which coincides with the strength of the vortex tube encircled by Γ, can be written in the form

$$\varphi_{\Gamma_L}(t) = \sum_{\Gamma} \delta\mathbf{l}_L(t) \cdot \mathbf{u}_L(t), \tag{9.5}$$

where the $\delta\mathbf{l}_L$ are infinitesimal elements of Γ_L. Differentiating in time Eq. (9.5) gives us

$$\begin{aligned} \dot{\varphi}_{\Gamma_L} &= \sum_{\Gamma} \mathbf{u}_L \cdot \frac{\mathrm{d}\delta\mathbf{l}_L}{\mathrm{d}t} + \sum_{\Gamma} \delta\mathbf{l}_L \dot{\mathbf{u}}_L \\ &= \sum_{\Gamma} \mathbf{u}_L \cdot \delta\mathbf{u}_L + \int_{\Gamma} \dot{\mathbf{u}}_L \cdot \mathrm{d}\mathbf{l}. \end{aligned} \tag{9.6}$$

From Euler's equation (5.28) we have

$$\dot{\mathbf{u}}_L = D_t\mathbf{u} = -\nabla(w - \Psi), \tag{9.7}$$

which, substituted into the last term in Eq. (9.6), gives us

$$\int_{\Gamma} \dot{\mathbf{u}}_L \cdot \mathrm{d}\mathbf{l} = -\int_{\Gamma} \mathrm{d}\mathbf{l} \cdot \nabla(w + \Psi) = 0. \tag{9.8}$$

where w is as usual the enthalpy per unit mass. In similar way we obtain for the remaing term in the last line of Eq. (9.6)

$$\sum_{\Gamma} \mathbf{u}_L \cdot \delta\mathbf{u}_L = \frac{1}{2} \sum_{\Gamma} \delta u_L^2 = 0, \tag{9.9}$$

which is a consequence of the fact that Γ is a closed curve, and the variation of u_L^2 around it is zero. We thus conclude

$$\varphi_{\Gamma_L} = \text{constant}. \tag{9.10}$$

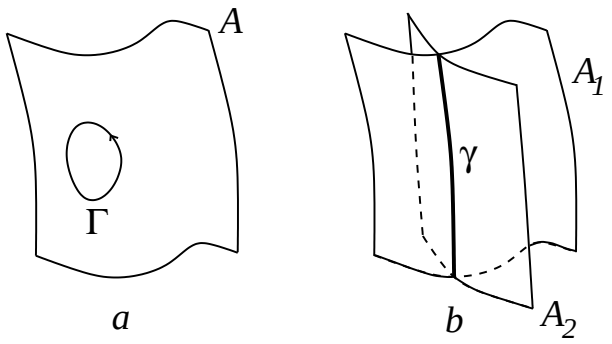

Figure 18: Representation of vortex sheets A, A_1 and A_2 and of the vortex line γ intersection of the two vortex sheets A_1 and A_2.

Kelvin's theorem has the important consequence that vortex lines are frozen in the flow. This is true because vortex sheets themselves are transported by the flow. The situation is illustrated in Fig. 18*a*. Suppose A is initially a vortex sheet, such as, e.g., the boundary of a vortex tube. Then, by construction, the vorticity flux Φ_Γ across any contour Γ on A is zero. As time passes, the points on A (and on Γ) are transported by the flow. By Kelvin's theorem, however, the flux Φ_{Γ_L} remains equal to zero. Since Γ is arbitrary, A_L then remains a vortex sheet.

We can verify that vorticity lines as well are transported by the flow. Consider the intersection γ of two vortex sheets S_1 and S_2 shown in Fig. 18. Vortex lines passing through points on γ are by construction simultaneously vortex lines of S_1 and S_2. However, the only line lying simultaneously in S_1 and S_2 is γ, which is therefore a vortex line.

The fact that vortex lines are frozen in the flow has important consequences on their topological properties. Since the strength of a vortex tube is constant along the tube and is conserved by the flow (if the latter is inviscid and barotropic), such a tube cannot be torn apart by the flow. Hence it must preserve its topology: if the tube is initially knotted it cannot unknot, vice-versa if it is initially unknotted.

Another consequence of the fact that vortex lines are transported by the flow is the phenomenon of vortex stretching. Due to the chaotic nature of most 3D flows, the separation of fluid elements will grow exponentially with time. Points along a vortex line will undergo the same process, and therefore the length of a vortex tube will itself grow exponentially with time. Now, unless the fluid is simultaneously undergoing an exponential expansion, the stretching process must be compensated by a simultaneous reduction in the section of the tube; this is particularly evident if the flow is incompressible, in which case the volume of the tube remains constant and the section A decreases exponentially. Since, by Kelvin's theorem, the strength of the tube remains constant, the vorticity in the tube must grow exponentially.

We can define the Reynolds number of a vortex tube of strength φ from Eq. (9.2), which gives us the velocity scale $U \sim \varphi/R$, where R is the instantaneous

radius of the vortex tube. This gives a value for the Reynolds number of the vortex tube

$$\mathrm{Re} \sim \frac{UR}{\nu} \sim \frac{\varphi}{\nu} = \text{constant}. \tag{9.11}$$

This would suggest that vortex stretching could go on forever, without viscosity setting in and causing the breakup of the vortex tube. This however is not true because as the vortex tube is stretched, it tends to fill densely the volume at its disposal, thus increasing the possibility of parts of the tube approaching other parts of that or other vortex tubes. Typically, during their interaction, the vortices end up rolling on one another, which leads to the formation of vortex sheets where the Reynolds number becomes very small. This in the end leads to the breakup of the flow topology (in place of a single closed vortex tube, we may be left with two or more vortex rings, knotted vortex tubes may unknot, etc.) and eventually to the destruction of the vortex structure.

Vortex stretching and the associated vorticity growth reflect the fact that the vorticity field is a frozen vector field, whose transport properties are described by the Lie derivative defined in Eq. (9.1). Vortex stretching in the expression

$$\mathcal{L}_{\mathbf{u}}\boldsymbol{\omega} = \mathbf{u} \cdot \nabla\boldsymbol{\omega} - \boldsymbol{\omega} \cdot \nabla\mathbf{u},$$

is accounted for by the term $-\boldsymbol{\omega} \cdot \nabla\mathbf{u}$, while $\mathbf{u} \cdot \nabla\boldsymbol{\omega}$ takes care of advection. In a reference frame moving locally with the fluid, we would have in fact

$$\dot{\boldsymbol{\omega}}_L = \boldsymbol{\omega} \cdot \nabla\mathbf{u}.$$

The situation is particularly transparent when $\boldsymbol{\omega}$ and $\mathbf{u}$ are parallel, in which case the growth of ω is precisely the local expansion rate of the flow.

9.2 Helicity conservation

The fact that the knottedness of the vortex lines in an inviscid and barotropic flow is conserved is reflected in the presence of a new conserved quantity called helicity. Let us focus for simplicity on the case of an infinite fluid, in which the vortex lines close on themselves. We can parameterize the knottedness of two vortex tubes γ_1 and γ_2 by the winding number $\alpha_{1,2}$, as illustrated in Fig. 19. Note that $\alpha_{1,2} = \alpha_{2,1}$. The helicity of the two vortex tubes is defined as

$$I_{1,2} = I_{2,1} = \alpha_{1,2}\varphi_1\varphi_2. \tag{9.12}$$

In particle physics, helicity is the projection of the spin onto the direction of the moment. The physical interpretation of helicity in the present fluid dynamics context is similar. Let us focus on vortex tube γ_1 and exploit Eq. (9.2) to express both φ_1

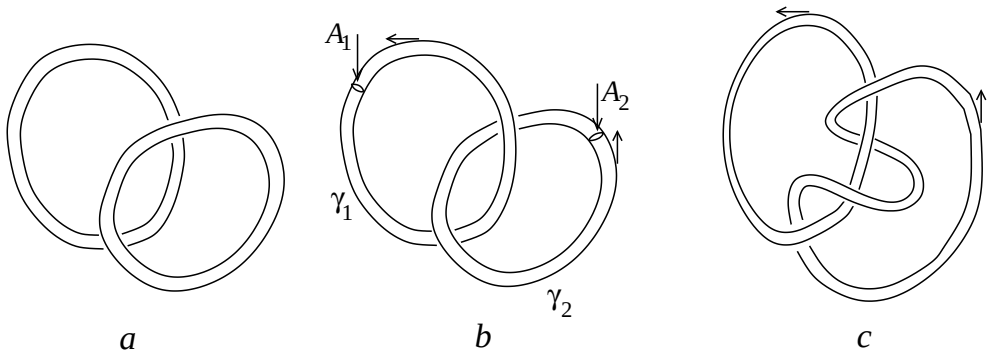

Figure 19: Degree of knottedness of vortex lines as a function of the winding number α. Arrows along the tubes indicate the orientations of $\boldsymbol{\omega}$. Case a: $\alpha = 0$; case b: $\alpha = 1$; case c: $\alpha = -2$. Note that the the winding number depends on the relative orientation of the vortex lines.

and φ_2 as integrals over γ_1: over the section S_1 in the case of φ_1; over the contour γ_1 in the case of φ_2:

$$\varphi_1 = \int_{A_1} \mathrm{d}\mathbf{A} \cdot \boldsymbol{\omega}, \qquad \varphi_2 = \int_{\gamma_1} \mathrm{d}\mathbf{l} \cdot \mathbf{u}, \tag{9.13}$$

where by construction $\boldsymbol{\omega}$ is parallel to both $\mathrm{d}A$ and $\mathrm{d}\mathbf{l}$ and $\boldsymbol{\omega} \cdot \mathrm{d}\mathbf{l} > 0$ and $\boldsymbol{\omega} \cdot \mathrm{d}\mathbf{A} > 0$. We find

$$I_{1,2} = \alpha_{1,2} \int_{A_1} \mathrm{d}\mathbf{A} \cdot \boldsymbol{\omega} \int_{\gamma_1} \mathrm{d}\mathbf{l} \cdot \mathbf{u} = \alpha_{1,2} \int_{V_1} \mathrm{d}\mathbf{A} \cdot \mathrm{d}\mathbf{l}\, \mathbf{u} \cdot \boldsymbol{\omega} = \alpha_{1,2} \int_{V_1} \mathrm{d}V\, \mathbf{u} \cdot \boldsymbol{\omega}. \tag{9.14}$$

Since φ_1, φ_2 and $\alpha_{1,2} = \alpha_{2,1}$ are simultaneously conserved in an inviscid fluid, also the helicity of the two vortex tubes will remain constant.

In the presence of more than two vortex tubes, the helicity of vortex tube γ_1 will be

$$I_1 = \sum_{j \neq 1} I_{1,j}, \tag{9.15}$$

leading to the total helicity in the fluid

$$I = \sum_{i \neq j} I_{i,j}. \tag{9.16}$$

We can now carry out a continuum limit and we get

$$I = \int \mathrm{d}V\, \mathbf{u} \cdot \boldsymbol{\omega}; \tag{9.17}$$

the velocity lines of a flow with non-zero helicity are locally helicoidal, which explains the name helicity for I.

Helicity in an inviscid fluid is globally conserved:

$$\dot{I} = 0; \tag{9.18}$$

an ideal fluid is therefore characterized by the presence of two quadratic invariants: total energy and total helicity. It turns out that helicity is also conserved in volumes V_L transported by the flow, provided $\boldsymbol{\omega}$ is locally tangent to the boundary of V_L; this means that vortex lines must neither enter nor exit V_L, and if V_L satisfies such property at an initial time, it will also satisfy it at later times. We can easily verify such property. If $\mathrm{d}\mathbf{A}$ is an element of ∂V_L with $\mathrm{d}\mathbf{A}\cdot\boldsymbol{\omega}|_{t=0} = 0$, by Kelvin's theorem, $\mathrm{d}\mathbf{A}\cdot\boldsymbol{\omega}|_{t>0} = 0$ as well. Vortex lines in V_L at $t = 0$ thus will remain in V_L also at a later time. The argument leading to helicity conservation for the vortex tubes in Eq. (9.14), therefore extends also to the vorticity in a volume transported by the flow. We thus obtain the local conservation law

$$\dot{I}_{V_L} = 0, \qquad \boldsymbol{\omega}\cdot\mathrm{d}\mathbf{A} = 0,\ \mathrm{d}\mathbf{A} \in \partial V_L. \tag{9.19}$$

Note that since we cannot send V_L to zero, the helicity density $\mathbf{u}\cdot\boldsymbol{\omega}$ is not a frozen field and therefore $D_t(\mathbf{u}\cdot\boldsymbol{\omega}) \neq 0$.

9.3 Two-dimensional flows

The vorticity dynamics of 2D flows, such as those in the atmosphere at scales much larger than the height of the troposphere, is qualitatively different from that in 3D. The crucial aspect is that, contrary to the 3D case, vorticity in two dimensions is by construction perpendicular to the velocity field. This implies that the vortex-stretching term $\boldsymbol{\omega}\cdot\nabla\mathbf{u}$ is absent in the vorticity evolution equation (9.1), and the topological constraints on the structure of vortex tubes thus disappear. This is reflected in the fact that the helicity of 2D flows is by construction equal to zero.

Equation (9.1) takes the form in two dimensions

$$D_t\boldsymbol{\omega} = -\nabla\times\frac{\nabla P}{\rho} + \nu\nabla^2\boldsymbol{\omega} + \nabla\times(\mathbf{f}^{ext}/\rho), \tag{9.20}$$

where $\boldsymbol{\omega}$ and the curls to RHS of the equation are perpendicular to the plane of the flow. To fix the ideas let us take $\boldsymbol{\omega} = (0, 0, \omega)$. If the flow is inviscid and barotropic and the external force per unit mass is curl-free, ω will behave like a frozen scalar,

$$D_t\omega = 0. \tag{9.21}$$

Equation (9.21) implies that the flow has a new infinite set of global invariants. Namely, the integral of any function of the vorticity weighed on the fluid density is a constant of the motion:

$$I_F = \int \mathrm{d}^2x\,\rho(\mathbf{x},t)F(\omega(\mathbf{x},t)) = \text{constant}; \tag{9.22}$$

we have in fact

$$\begin{aligned}
\dot{I}_F &= \int \mathrm{d}^2x \left[F\partial_t\rho + \rho F'\partial_t\omega \right] \\
&= -\int \mathrm{d}^2x \left[F\nabla\cdot(\rho\mathbf{u}) + \rho F'\mathbf{u}\cdot\nabla\omega \right] \\
&= -\int \mathrm{d}^2x \left[F\nabla\cdot(\rho\mathbf{u}) + \rho\mathbf{u}\cdot\nabla F \right] \\
&= -\int \mathrm{d}^2x\, \nabla\cdot(\rho F\mathbf{u}) = 0.
\end{aligned} \tag{9.23}$$

We note that this property is shared by any frozen scalar, such as, e.g., temperature in the absence of diffusion.

The following quadratic invariant is called enstrophy,

$$\mathcal{E} = \frac{1}{2}\int \mathrm{d}^2x\, \rho\omega^2 = \text{constant}. \tag{9.24}$$

In the presence of a finite viscosity, the quantities I_F will not be conserved. In particular we can easily derive an equation for the viscous dissipation of enstrophy

$$\dot{\mathcal{E}} = -\int \mathrm{d}^2x\, \mu|\nabla\omega|^2, \tag{9.25}$$

which is perfectly analogous to Eq. (5.4). We note that, contrary to helicity, enstrophy is the integral of a positive quantity, so that enstrophy conservation cannot be satisfied by balancing contributions with different signs in the integral in Eq. (9.24); this makes the global constraint on enstropphy more severe than the one on helicity; we shall return on this point when discussing 2D turbulence.

9.4 Invariance under relabeling

Conserved quantities in conservative systems are associated, through Noether's theorem, with the existence of symmetries. Inviscid fluids make no exception: energy conservation is associated with invariance under time translation; linear and angular momentum conservation is associated with invariance under translation and rotation. We are going to show that Kelvin's theorem and the various conservation laws with which it is associated stem from symmetry under relabeling of the fluid trajectories.

An inviscid fluid is basically an ensemble of fluid elements moving under the action of pressure and external forces. Let us neglect for simplicity the effect of external forces and assume barotropic conditions. This means that the internal energy density of the fluid is in the form

$$\mathcal{E} = c_V P(\rho). \tag{9.26}$$

The total energy of the system is equal to the sum of the kinetic energy of the fluid elements and of a potential energy term that can be identified with the volume integral of $\mathcal{E}$. The role of the variables $q_i(t)$ in the Lagrangian of a mechanical system is taken here by the Lagrangian coordinates of the fluid elements $\mathbf{x}_L(t|\mathbf{y}, t_0)$, in which the continuous label $\mathbf{y}$ takes the place of the discrete index i. We have already pointed out that the choice of the label is arbitrary. So far we have interpreted $\mathbf{y}$ as an initial condition, $\mathbf{y} \equiv \mathbf{x}_0 = \mathbf{x}_L(t_0|\mathbf{x}_0, t_0)$; it is convenient to carry out the present analysis in a generic compressible case; we thus choose to deform the coordinates $\mathbf{x}_0$ associated with the initial conditions for $\mathbf{x}_L$, into new coordinates $\mathbf{y}$ such that

$$\rho(\mathbf{x}_0, t_0)\mathrm{d}^3x_0 = \mathrm{d}^3y = \mathrm{d}M \tag{9.27}$$

is the mass of the fluid element; this allows us to write the density at time t in terms of the Jacobian $J(\mathbf{y}, t)$ of the transformation $\mathbf{y} \to \mathbf{x}_L$:

$$\rho(\mathbf{x}_L, t) = \left|\left|\frac{\partial \mathbf{x}_L}{\partial \mathbf{y}}\right|\right|^{-1} := J(\mathbf{y}, t). \tag{9.28}$$

The action of the fluid takes then the form:

$$\mathcal{A} = \int \mathrm{d}t\, L[u_L, P; t] = \int \mathrm{d}t \int \mathrm{d}^3y \left[\frac{1}{2}u_L^2(\mathbf{y}, t) - c_V P(J(\mathbf{y}, t))\right]. \tag{9.29}$$

A simple example of relabeling is the shift $\mathbf{y} \to \mathbf{y}' = \mathbf{y} + \delta\mathbf{y}(\mathbf{y})$. To obtain Kelvin's theorem, however, we must require invariance with respect to a larger class of time-dependent reparameterizations

$$\mathbf{y} \to \mathbf{y}' = \mathbf{y} + \delta\mathbf{y}(\mathbf{y}, t). \tag{9.30}$$

We require that the shift $\mathbf{y} \to \mathbf{y}'$ still satisfies Eq. (9.27), $\mathrm{d}^3y = \mathrm{d}^3y' = \mathrm{d}M$, which implies

$$\nabla_y \cdot \delta\mathbf{y} = 0 \Rightarrow \delta J = 0. \tag{9.31}$$

After the shift in Eq. (9.30), a single $\mathbf{y}$ will then be associated, at different times, with different trajectories.

Evaluation of $\delta\mathcal{A}$ is simplified by Eq. (9.31), which tells us that the variation of P in $\delta\mathcal{A}$ is zero. We thus get

$$\delta\mathcal{A} = \frac{1}{2}\int \mathrm{d}t \int \mathrm{d}^3y\, \delta u_L^2(t|\mathbf{y}, t_0) = \int \mathrm{d}t \int \mathrm{d}^3y\, \mathbf{u}_L \cdot \delta\mathbf{u}_L. \tag{9.32}$$

To express $\delta\mathbf{u}_L$ in terms of the shift $\delta\mathbf{y}$, we exploit the construction in Fig. 20 which allows us to write

$$\begin{aligned}
\mathbf{u}_L(t|\mathbf{y}, t_0) &= \lim_{\delta t\to 0} \frac{\mathbf{x}_L(t|\mathbf{y}_a, t_0) - \mathbf{x}_L(t-\delta t|\mathbf{y}_a, t_0)}{\delta t} \\
&= \lim_{\delta t\to 0} \frac{\mathbf{x}_L(t|\mathbf{y}_a, t_0) - \mathbf{x}_L(t|\mathbf{y}_b, t_0)}{\delta t} \\
&= \lim_{\delta t\to 0} \frac{\mathbf{x}_L(t|\mathbf{y}_L(x_c, t-\delta t), t_0) - \mathbf{x}_L(t|\mathbf{y}_L(\mathbf{x}_c, t), t_0)}{\delta t} \\
&= -\mathbf{v}(\mathbf{y}, t) \cdot \nabla_y \mathbf{x}_L(t|\mathbf{y}, t_0),
\end{aligned} \tag{9.33}$$

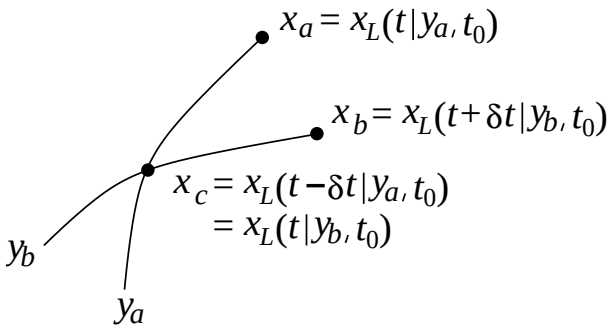

Figure 20: Lagrangian trajectories and their relative labels $\mathbf{y}_a$ and $\mathbf{y}_b$.

where $\mathbf{y}_L(\mathbf{x},t) \equiv \mathbf{y}_L(t_0|\mathbf{x},t)$, and where we have introduced the velocity in $\mathbf{y}$-space

$$\mathbf{v}(\mathbf{y},t) = \lim_{\delta t\to 0} \frac{\mathbf{y}_L(\mathbf{x}_L(\mathbf{y},t),t) - \mathbf{y}_L(\mathbf{x}_L(\mathbf{y},t),t-\delta t)}{\delta t}. \tag{9.34}$$

The variation of $\mathbf{u}_L(t|\mathbf{y},t_0)$ reads

$$\begin{aligned} \delta\mathbf{u}_L &= -(\delta\mathbf{v}_L)\cdot\nabla_{\mathbf{y}}\mathbf{x}_L - (\mathbf{v}_L)\delta\mathbf{y} : \nabla_y\nabla_y\mathbf{x}_L. \\ &= -(\delta\mathbf{v}_L)\cdot\nabla_{\mathbf{y}}\mathbf{x}_L + \delta\mathbf{y}\cdot\nabla_y\mathbf{u}_L, \end{aligned} \tag{9.35}$$

where to go to the second line of the equation, we have exploited Eq. (9.33); we recall that $\delta\mathbf{y} = \delta\mathbf{y}(\mathbf{y},t)$.

We can now substitute Eq. (9.35) into Eq. (9.32); we get

$$\begin{aligned} \delta\mathcal{A} &= \int \mathrm{d}t \int \mathrm{d}^3y \left\{ -\mathbf{u}_L\cdot[\delta\mathbf{v}\cdot\nabla_{\mathbf{y}}\mathbf{x}_L] + \frac{1}{2}\delta\mathbf{y}\cdot\nabla_y u_L^2 \right\} \\ &= -\int \mathrm{d}t \int \mathrm{d}^3y\, \mathbf{A}\cdot\delta\mathbf{v}, \end{aligned} \tag{9.36}$$

where we have defined

$$\mathbf{A} = u_{L_i}\nabla_y x_{Li}, \tag{9.37}$$

and to proceed to the second line of the Eq. (9.36), we have integrated by parts with respect to y the term $\delta\mathbf{y}\cdot\nabla_y u_L^2$, and then exploited Eq. (9.31). We next integrate by part with respect to t and we get

$$\delta\mathcal{A} = \int_{t_i}^{t_f} \mathrm{d}t \int \mathrm{d}^3y\, \delta\mathbf{y}\cdot\partial_t\mathbf{A}. \tag{9.38}$$

Now, the volume preservation condition in Eq. (9.31) implies that $\delta\mathbf{y}$ is the curl of some vector field $\mathbf{T}$:

$$\delta\mathbf{y}(\mathbf{y},t) = \nabla_y\times\mathbf{T}(\mathbf{y},t). \tag{9.39}$$

Substituting Eq. (9.39) into Eq. (9.38) and integrating by parts with respect to y yields then the final expression

$$\delta\mathcal{A} = \int_{t_i}^{t_f} \mathrm{d}t \int \mathrm{d}^3 y\, \mathbf{T} \cdot \partial_t [\nabla_y \times \mathbf{A}]. \tag{9.40}$$

The remaining steps are straightforward. Invariance under relabeling means that the variation of $\mathcal{A}$ with respect to $\delta\mathbf{y}$ is zero. Since $\mathbf{T}$ is arbitrary, $\partial_t[\nabla_y \times \mathbf{A}] = 0$, which implies that the circulation of $\mathbf{A}$ around an arbitrary path Γ_y in $\mathbf{y}$-space is constant:

$$\int_{\Gamma_y} \mathrm{d}\mathbf{y} \cdot \mathbf{A} = \text{constant}. \tag{9.41}$$

However, from Eq. (9.37), $\mathbf{A} \cdot \mathrm{d}\mathbf{y} = \mathbf{u}_L \cdot \mathrm{d}\mathbf{x}$. From Eq. (9.40) we thus recover the statement in Kelvin's theorem

$$\int_{\Gamma_L} \mathrm{d}\mathbf{l} \cdot \mathbf{u} = \text{constant}. \tag{9.42}$$

9.5 Suggested reading

- J. Pedlosky, "Geophysical fluid mechanics", Chap. 7, (Springer 1987)
- R. Salmon, "Hamiltonian fluid mechanics", Annu. Rev. Fluid Mech. pp. 225 vol 20 (1988)

10 Turbulence

High Reynolds number flows are usually turbulent. The interaction of the fluid with a solid obstacle leads, because of the no-slip boundary condition, to the formation of vortex sheets which are structurally unstable, roll into vortex tubes that are continuously stretched and deformed and lead to the formation of small-scale turbulent structures. A flow that is initially at spatial scale L thus breaks into a multitude of eddies at scales $l \ll L$. The energy of the mean flow is continuously transferred to the turbulent fluctuations, and the energy of the smallest eddies is converted to heat through viscous dissipation. This suggests us that a satisfactory description of the turbulent dynamics could be achieved by writing evolution equations for the mean velocity of the flow, $\bar{\mathbf{u}}(\mathbf{x}, t)$, and the turbulent kinetic energy and viscous dissipation.

Since most of the difficulties of turbulence are already present in incompressible flows, we assume incompressibility from the start. The turbulent energy and dissipation per unit mass read

$$k(\mathbf{x}, t) = \frac{1}{2}\overline{\tilde{u}^2(\mathbf{x}, t)}, \qquad \epsilon(\mathbf{x}, t) = \frac{\nu}{2}\overline{||\tilde{\mathbf{s}}(\mathbf{x}, t)||^2}, \tag{10.1}$$

where we use tilde to identify fluctuations.

The turbulent vortices are transported by the mean flow and by turbulence. An equation for the mean flow can be obtained directly as the average of the Navier-Stokes equation (4.4):

$$\rho \bar{D}_t \bar{\mathbf{u}} + \nabla \bar{P} = \mathbf{f}^{ext} + \nabla \cdot (\mu \nabla \bar{\mathbf{u}} - \rho \overline{\tilde{\mathbf{u}}\tilde{\mathbf{u}}}), \tag{10.2}$$

where $\bar{D}_t = \partial_t + \bar{\mathbf{u}} \cdot \nabla$. Note the quadratic term to RHS, which contains the effect of random advection by the turbulent eddies: $\nabla \cdot \overline{\tilde{\mathbf{u}}\tilde{\mathbf{u}}} = D_t \mathbf{u} - \bar{D}_t \bar{\mathbf{u}}$. To solve Eq. (10.2) we need an expression for the quadratic average $\overline{\tilde{\mathbf{u}}\tilde{\mathbf{u}}}$. We immediately realize that since there are six independent components in $\overline{\tilde{\mathbf{u}}\tilde{\mathbf{u}}}$, solving an equation for k is not enough. More seriously, in the same way the equation for $\bar{\mathbf{u}}$ contains through advection a quadratic contribution $\overline{\tilde{\mathbf{u}}\tilde{\mathbf{u}}}$, an equation for $\overline{\tilde{\mathbf{u}}\tilde{\mathbf{u}}}$ will involve a cubic component $\overline{\tilde{\mathbf{u}}\tilde{\mathbf{u}}\tilde{\mathbf{u}}}$. A similar situation would occur if we tried to write an equation for the cubic term, and so on. The result is an infinite system of coupled equations which can realistically be solved only by assuming in some equations a specific form of the highest order correlations.

A possible strategy is to exploit the analogy between the Reynolds stress and the viscous stress, and introduce an eddy viscosity μ_T, in which the characteristic size L of the eddies and their characteristic velocity $\tilde{u}_L$ take the place of the mean free path λ and the thermal velocity v_{th} in μ (see Eq. (4.16). The result is

$$R_{ij} = \nu_T \overline{\dot{s}_{ij}}, \qquad \nu_T = \tilde{u}_L L. \tag{10.3}$$

where

$$\tilde{u}_L \sim \sqrt{k}, \tag{10.4}$$

and L is the characteristic scale of the largest eddies in the particular region of the flow. Thus, in the same way molecular motion leads to diffusion of momentum and scalar quantities such as the temperature, one may imagine that the same effect in turbulence is produced by the individual eddies. A value of L can be estimated by assuming some sort of local equilibrium between the power delivered by the advection force by the largest eddies, $\rho\tilde{\mathbf{u}}\cdot(\tilde{\mathbf{u}}\cdot\nabla)\tilde{\mathbf{u}}\sim\tilde{u}_L^3/L$, and the dissipation rate ϵ:

$$L\sim\frac{k^{3/2}}{\epsilon}\Rightarrow\nu_T\sim\frac{k^2}{\epsilon}. \tag{10.5}$$

Typically, one reabsorbs the molecular viscosity in ν_T, $\nu+\nu_T\to\nu_T$ and Eq. (10.2) takes the form

$$\rho\bar{D}_t\bar{u}_i+\partial_i\bar{P}=f_i^{ext}+\partial_j(\mu_T\partial_j\bar{u}_i),\qquad\mu_T=\rho\nu_T. \tag{10.6}$$

The turbulent viscosity μ_T plays a fundamental role in the energy budget of the flow. While in the case of molecular viscosity, the energy of the flow was directly converted to heat, the eddy viscosity transfers energy from the mean flow to the turbulent fluctuations. One can get some intuitive understanding of the mechanism by referring to the concept of added mass introduced in Sec. 8.2; this is the mass of the fluid that a solid object drags along in its motion. Turbulent eddies continuously replace chunks of the moving fluid with other fluid masses that have initially zero velocity. The work required to overcome the viscous drag and keep the body in motion is then precisely the work required to accelerate those masses to the speed of the body.

We can exploit the concept of eddy viscosity to derive an effective equation for the transport of k. The structure of the equation is very similar to that of the heat transport equation (5.6), with eddy diffusion of k replacing molecular diffusion of T and turbulent energy production from the work against the turbulent stress replacing viscous heating. The result is

$$\bar{D}_tk=\nabla\cdot(\nu_T\nabla k)+2\nu_T||\bar{\mathbf{s}}||^2-\epsilon, \tag{10.7}$$

We can derive a similar equation for ϵ:

$$\bar{D}_t\epsilon=\nabla\cdot(\nu_T^\epsilon\nabla\epsilon)+\frac{c\epsilon}{k}[2\nu_T^\epsilon||\bar{\mathbf{s}}||^2-\epsilon],\qquad\nu_T^\epsilon\sim\nu_T,\quad\nu_T^\epsilon\sim\nu_T,\quad c\sim1. \tag{10.8}$$

Equations (10.6-10.8) constitute the so-called $k-\epsilon$ model of turbulence.

Building something that goes beyond an empirical model of turbulence appears at the present state of knowledge a very difficult task. Perturbative treatment of the equation, in particular, does not work (such an approach would correspond to expand around a lowest-order $\mathrm{Re}\to0$ dynamics that has no relation with turbulence). On the other hand, brute force numerical simulation of the Navier-Stokes equation is usually unfeasible (an atmospheric flow may involve eddies ranging from hundreds

of meters to the millimeter scale). There are alternative approaches in which the Navier-Stokes equation is numerically solved with a grid scale that excludes the smallest eddies in the flow (large-eddy simulations or LES). As in the case of the $k-\epsilon$ model, the effect of the unresolved eddies is modeled by introducing an eddy viscosity $\nu_T \sim l_{grid}\tilde{u}_{subgrid}$, in which the large scale L and the turbulent velocity $\tilde{u}_L$ are replaced by the scale of the grid l_{grid} and the characteristic velocity $\tilde{u}_{subgrid}$ of the unresolved eddies; both quantities l_{grid} and $\tilde{u}_{subgrid}$ must in some way be parameterized.

10.1 Homogeneous isotropic turbulence

Turbulence is spatially inhomogeneous almost by definition. The inhomogeneity scale is fixed by the geometry of the problem: in the case of a turbulent pipe flow, the diameter of the pipe; in the case of a turbulent wake downstream of a solid body, the width of the wake; in the case of a flow over a plane surface, the thickness of the boundary layer. The inhomogeneity scale itself may vary with the position (the distance downstream of the solid obstacle or along the plane surface).

Typically, the characteristic scale of the mean flow and the size L of the largest eddies are comparable:

$$L \sim \bar{u}/\partial_x \bar{u}, \tag{10.9}$$

and the statistics of the large eddies are in general neither spatially homogeneous nor isotropic. Nevertheless, if the turbulence is sufficiently strong, eddies at scales $l \ll L$ will be present, which will see turbulence as locally homogeneous and isotropic. Furthermore, since the dynamics of smaller eddies is faster than that of larger eddies, their statistics can be assumed to be stationary.

A necessary condition for isotropy is that the strain on eddies at scale $l \ll L$ mainly comes from eddies of comparable scale. In other words, the turbulent dynamics at a sufficiently small scale must be local in scale. We want in particular that the strain on eddies at scale $l \ll L$ from eddies at scale L and from the mean flow (which are both anisotropic) be negligible.

We can identify in a turbulent flow three ranges of scales:

- An integral scale L of large eddies which interact directly with the mean flow and are sensitive to the geometry of the flow domain.
- An internal scale η of the smallest eddies, for which $Re_\eta = \eta\tilde{u}_\eta/\nu \lesssim 1$ and the effect of viscosity is dominant.
- An intermediate "inertial" range $L \ll l \ll \eta$ in which eddies are sufficiently small for hypotheses of homogeneity and isotropy to hold, and at the same time sufficiently large for the dynamics to be inviscid.

Kolmogorov was able, based on such simple hypotheses, to derive the energy spectrum in the inertial range of turbulence and an expression for the internal scale η. The simplest derivation only requires dimensional analysis, based on the hypothesis of self-simiilarity and independence of the inertial range dynamics on viscosity. Such hypothesis contain in a subtle way the condition that small-scale turbulent fluctuations are sufficiently random and organized small-scale structures do not create bottlenecks in the energy transfer. We can get an insight into the physics underlying the Kolmogorov theory by looking at the dynamics of a single vortex at scale l.

If vortices are distributed uniformly in the flow domain, the contribution to the turbulent energy density by eddies at scale l will be $k_l \sim \tilde{u}_l^2$. Vortex stretching transforms vortices at scale l into vortices at scale, say, $l/2$ in a characteristic time τ_l, which, if the process is dominated by vortices of comparable size, will coincide with the eddy turnover time

$$\tau_l \sim l/\tilde{u}_l. \tag{10.10}$$

We can visualize the process as a turbulent cascade in which energy is transferred from eddies at scale L to eddies at scale $L/2$, and from there to smaller eddies until one reaches the internal scale η. Now, for the process to be stationary, the energy flux from one scale to the next must be scale-independent and equal viscous dissipation:

$$\Pi_l \sim \frac{k_l}{\tau_l} \sim \frac{\tilde{u}_l^2}{\tau_l} = \Pi = \epsilon. \tag{10.11}$$

From Eqs. (10.10) and (10.11) we then get the scaling law (Kolmogorov scaling)

$$\tilde{u}_l \sim (\epsilon l)^{1/3}. \tag{10.12}$$

We can now verify that the contribution to the velocity increment $\tilde{\mathbf{u}}(\mathbf{x}+\mathbf{l},t) - \tilde{\mathbf{u}}(\mathbf{x},t)$ from eddies at scale l is indeed the largest. We verify immediately that the contribution of vortices with $l' \ll l$ is $\tilde{u}_{l'} \sim \tilde{u}_l (l'/l)^{1/3} \ll u_l$. On the other hand, if we imagine the eddies to be smooth objects, such that their velocity field can be Taylor expanded, the contribution to $\Delta_{\mathbf{l}}\tilde{\mathbf{u}}(\mathbf{x},t) = \tilde{\mathbf{u}}(\mathbf{x}+\mathbf{l},t) - \tilde{\mathbf{u}}(\mathbf{x},t)$ from eddies with $l' \gg l$ will be $\sim \tilde{u}_{l'} l/l' \sim \tilde{u}_l (l/l')^{2/3} \ll \tilde{u}_l$. Now, stretching of vortices at scale l is produced by velocity differences at separation l; the fact that the difference $\Delta_{\mathbf{l}}\tilde{\mathbf{u}}(\mathbf{x},t)$ is dominated by eddies of size l then confirms the picture of local energy transfer in scale as the result of the interaction of vortices of comparable size.

The fact that the difference $\Delta_{\mathbf{l}}\tilde{\mathbf{u}}(\mathbf{x},t)$ is dominated by eddies of size l allows us to write Eq. (10.12) in the equivalent form

$$\overline{|\tilde{\mathbf{u}}(\mathbf{x}+\mathbf{l},t) - \tilde{\mathbf{u}}(\mathbf{x},t)|^2} \sim \epsilon^{2/3} l^{2/3}, \tag{10.13}$$

which tells us that for $\eta \to 0$ the turbulent velocity field becomes non-differentiable in space. The velocity field itself, however, remains finite and the same property is

shared by the turbulent kinetic energy:

$$k = \sum_{n=0}^{+\infty} k_n \sim \sum_{n=0}^{+\infty} \tilde{u}_{l_n}^2/2 < \infty, \qquad l_n = 2^{-n}L. \tag{10.14}$$

We can use Eq. (10.12) to evaluate the internal scale η. Proceeding as in the case of the turbulent energy, the viscous dissipation ϵ can be expressed as a sum of contributions by vortices at different scales. We see from Eq. (10.12), that the sum is dominated by eddies at scale $\eta := L2^{n_\eta}$:

$$\epsilon = 2\nu\overline{|\nabla \mathbf{u}|^2} \sim \nu \sum_n \tilde{u}_{l_n}^2 l_n^2 \sim \nu\epsilon^{2/3}L^{-4/3}\sum_{n=0}^{n_\eta} 2^{4n/3} \sim \nu\epsilon^{2/3}\eta^{-4/3}. \tag{10.15}$$

From here we obtain

$$\eta \sim \nu^{3/4}\epsilon^{-1/4}, \tag{10.16}$$

which is called the Kolmogorov scale of the flow. At scales below η the flow is dominated by viscosity and could be described using the Stokes equation (8.1). We can then verify that for $l < \eta$, $\overline{|\tilde{\mathbf{u}}(\mathbf{x}+\mathbf{l},t) - \tilde{\mathbf{u}}(\mathbf{x},t)|^2} \sim l^2$; in other words, the turbulent velocity field at sufficiently small scale is smooth.

From Eqs. (10.10) and (10.13) we get the scaling for the eddy turnover time

$$\tau_l \sim \epsilon^{-1/3} l^{2/3}. \tag{10.17}$$

The time required for vortex stretching from L to η to complete is

$$\tau_{L\to\eta} \sim \sum_n \tau_{L2^{-n}} \sim \tau_L \sum_n 2^{-2n/3} \sim \tau_L, \tag{10.18}$$

independent of ν, which implies that the times required in the $\nu \to 0$ limit to reduce integral scale vortices to infinitesimal smithereens remains finite.

We can take the limit $l \to L$ in Eq. (10.13) and express the viscous dissipation in terms of properties of the large scale flow:

$$\epsilon \sim \frac{\tilde{u}_L^3}{L}. \tag{10.19}$$

We find again the result that viscous dissipation remains finite in the $\nu \to 0$ limit; the only thing that changes is the Kolmogorov scale that goes to zero. By substituting Eq. (10.19) into Eq. (10.16) we are able to write the ratio L/η of the maximum and minimum scale in the turbulent flow in terms of the Reynolds number:

$$\frac{L}{\eta} \sim \left(\frac{L\tilde{u}_L}{\nu}\right)^{4/3} = \mathrm{Re}^{4/3}, \tag{10.20}$$

which allows us to estimate the number of grid points required in a numerical simulation of a turbulent flow as $\sim \mathrm{Re}^4$.

10.1.1 Time structure of the inertial range

The Kolmogorov law, Eq. (10.13), gives us information on the spatial structure of the turbulent flow. The temporal structure is much more intricate; this turns out to be one of the major stumbling blocks in the derivation of a theory of turbulence. The fact is that the eddy turnover time τ_l defined in Eq. (10.10) describes the time decay of correlations in a reference frame moving with the fluid, i.e. the decay of Lagrangian time correlations. Eulerian time correlations will be affected by the transport of eddies by larger eddies and the mean flow—a phenomenon called sweep effect.

The magnitude of the sweep effect is determined by the transit time of the vortices in front of a fixed probe; in the case of vortices of size l:

$$\tau_l^E \sim l/u \sim l/\bar{u}. \tag{10.21}$$

We see from Eqs. (10.17) and (10.21) that for $l \ll L$, $\tau_l^E \ll \tau_l$; this tells us that vortex stretching, although crucial for the dynamics of the flow, only contributes a correction to Eulerian correlations.

The fact that the turbulent dynamics is properly described only in a Lagrangian frame, enormously complicates the derivation of a theory of turbulence based on the Navier-Stokes equation. The fact that vortices at scale l can be approximated as frozen on the time scale of τ_l^E, however, simplifies experimental measurements. We can in fact approximate

$$\mathbf{u}(\mathbf{x}, t) - \mathbf{u}(\mathbf{x}, 0) \simeq \mathbf{u}(\mathbf{x} - \bar{\mathbf{u}}t, 0) - \mathbf{u}(\mathbf{x}, 0), \qquad t \ll L/\bar{u} \sim \tau_L, \tag{10.22}$$

which is called Taylor's frozen-turbulence approximation. Equation (10.22) tells us that it is possible to reconstruct an instantaneous spatial section of a turbulent flow from the time series of the velocities measured by a fixed probe (an anemometer).

10.1.2 Transport of a passive scalar

The heat transport equation (5.10) is the first example of transport equation for a scalar quantity we have considered in these notes; in the case of an incompressible flow, it takes the form

$$D_t T = \kappa \nabla^2 T + h, \tag{10.23}$$

where h is a generic source term. The transport of a substance, such as e.g. a pollutant in the air, will obey an equation of identical form, with T identifying in this case the substance concentration. If there is no feedback on the flow (in the case of the temperature, this means that convection is negligible), we say that T behaves like a passive scalar.

We want to study passive scalar transport by turbulence. Suppose we have a localized heat source h that generates an inhomogenous temperature profile in the

surroundings. An inhomogeneous time-dependent but non-turbulent flow is sufficient to generate mixing; turbulence contributes to the process, with many characteristics in common with the turbulent cascade of velocity fluctuations previosly discussed: large scale inhomogeneities in T are generated by the source h and converted to smaller and smaller scales fluctuations which are eventually smoothed out by diffusion. We will have an integral scale L_T where the effect of the flow geometry and the source h are substantial, followed by an inertial range where both h and κ play a negligible role, and an internal scale η_T where diffusion is dominant.

Let us focus on the inertial range. From Eq. (10.23) fluctuations at scales $\eta_T \ll l \ll L_T$ behave like a frozen field. We have seen, when studying the dynamics of vorticity in 2D flows (see Sec. 9.3), that a frozen scalar has an infinite set of global invariant

$$\int \mathrm{d}^3x\, F(T(\mathbf{x},t)) = \text{constant},\ \forall F. \tag{10.24}$$

In particular, we have a quadratic invariant

$$k_T = \frac{1}{2}\int \mathrm{d}^3x\, T^2(\mathbf{x},t), \tag{10.25}$$

which behaves like a sort of energy of the temperature fluctuations. We can then repeat the same steps in the case of the velocity fluctuations and introduce a flux in scale of the temperature fluctuations

$$\Pi_l^T \sim \frac{\tilde{T}_l^2}{\tau_l} \sim \epsilon^{1/3} l^{-2/3} \tilde{T}_l^2 \sim \epsilon_T, \tag{10.26}$$

where

$$\epsilon_T = \kappa \overline{|\nabla T|^2} \sim \kappa \frac{\tilde{T}_{\eta_T}^2}{\eta_T^2} \tag{10.27}$$

is the dissipation of temperature fluctuations by diffusion. Proceeding as in the case of the velocity fluctuations we get

$$\overline{|\tilde{T}(\mathbf{x}+\mathbf{l},t) - \tilde{T}(\mathbf{x},t)|^2} \sim \epsilon_T \epsilon^{-1/3} l^{2/3} \tag{10.28}$$

and in the case $\nu \sim \kappa$

$$\eta_T \sim \kappa^{3/4} \epsilon^{-1/4}. \tag{10.29}$$

Experiments and numerical simulations support Kolmogorov scaling both for the velocity and passive scalar field. There are corrections, whose existence is confirmed by mathematical analysis of Eq. (10.23). The smallness of the corrections, however, suggests that the Kolmogorov cascade picture is correct and the role of the infinite set of conserved quantities in Eq. (10.24) is small.

A possible explanation of why higher-order invariants can be disregarded is that only $F(T) = T^2/2$ can be decomposed as a sum of scale-dependent terms. To see why this is the case, it is necessary to work in Fourier space:

$$\tilde{T}_{\mathbf{k}}(t) = \int \mathrm{d}^3x\, T(\mathbf{x},t)\mathrm{e}^{-\mathrm{i}\mathbf{k}\cdot\mathbf{x}}. \tag{10.30}$$

Let us consider the case F is a simple power of T (which covers the case F is regular in $T = 0$ and can therefore be expressed as a Taylor series in T). We have

$$\begin{aligned} I_n = \int \mathrm{d}^3x\, \overline{\tilde{T}^n} &= \int \mathrm{d}^3x \int \prod_{j=1}^{n} \frac{\mathrm{d}^3k_j}{(2\pi)^3} \overline{\tilde{T}_{\mathbf{k}_1} \dots \tilde{T}_{\mathbf{k}_n}} \exp\Big(-\mathrm{i}\mathbf{x}\cdot\sum_{j=1}^{n}\mathbf{k}_j\Big) \\ &= (2\pi)^3 \int \prod_{j=1}^{n} \frac{\mathrm{d}^3k_j}{(2\pi)^3} \overline{\tilde{T}_{\mathbf{k}_1} \dots \tilde{T}_{\mathbf{k}_n}} \delta\Big(\sum_{j=1}^{n}\mathbf{k}_j\Big). \end{aligned} \tag{10.31}$$

As claimed, only I_2 is a sum of contributions dependent on a unique scale k^{-1}:

$$I_2 = \int \frac{\mathrm{d}^3k}{(2\pi)^3} \overline{|\tilde{T}_{\mathbf{k}}|^2}. \tag{10.32}$$

In all other cases, the integrand of I_n depends on more than one wavevector, and there will be contributions in which some of the wavevectors lie out of the inertial range. For such contributions, local transfer in scale of a conserved quantity could not be invoked.

10.1.3 Two-dimensional turbulence

The mechanism of vortex stretching, which determines the dynamics of turbulence in three dimensions, is absent in two dimensions. Another difference with the 3D case is the presence of a second quadratic invariant, enstrophy, which leads to the question of whether energy or enstrophy determines the structure of the turbulent cascade. Also in three dimensions there is a second quadratic invariant, helicity; however, while zero enstrophy would require a flow that is globally potential (and therefore non-turbulent), in order to have zero helicity it is sufficient that the flow is globally reflection invariant. Thus, while an energy k_l at scale l implies an enstrophy content at that scale $\mathcal{E}_l \sim k_l/l^2$, in the case of helicity we can only state $|I_l| \lesssim k_l/l$.

With all the caveats put in place, let us try to understand whether a local turbulent cascade is possible in two dimensions. Let us start by considering the possibility of an enstrophy cascade and define an enstrophy flux $\Pi_{\mathcal{E},l}$ and an enstrophy dissipation $\epsilon_{\mathcal{E}}$, which at stationarity are going to be equal. The same argument leading to the Kolmogorov scaling in Eq. (10.13) yields in the present case

$$\epsilon_{\mathcal{E}} \sim \frac{\mathcal{E}_l}{\tau_l} \sim \frac{\tilde{u}_l^3}{l^3} \Rightarrow \tilde{u}_l \sim \epsilon_{\mathcal{E}}^{1/3} l; \tag{10.33}$$

enstrophy dissipation equals the enstrophy injection, which is $\sim L^{-2}$ times the energy injection; hence $\epsilon_{\mathcal{E}} \sim \epsilon/L^2$.

We immediately find a difficulty in the fact that the scaling $\tilde{u}_l \propto l$ implies that the contribution to $\Delta_{\mathbf{l}}\tilde{\mathbf{u}}(\mathbf{x},t) = \tilde{\mathbf{u}}(\mathbf{x}+\mathbf{l},t) - \tilde{\mathbf{u}}(\mathbf{x},t)$ from vortices at scale $l' \gg l$ is of the same order as that of vortices at scale l. This clearly weakens a hypothesis of local enstrophy transfer in scale. A more substantial difficulty is that energy is injected in the flow side by side with enstrophy. However, while $\Pi_{\mathcal{E},l} = \epsilon_{\mathcal{E}}$ is constant, $\Pi_{k,l} \equiv \Pi_l \sim \epsilon_{\mathcal{E}} l^2$ goes to zero for $l \to 0$. Stationarity then requires that $\Pi_l = 0$ independent of scale. The alternative in which the dynamics is governed by energy transfer and $\tilde{u}_l \sim (\epsilon l)^{1/3}$ as in Eq (10.12) is not viable since it would lead to $\Pi_{\mathcal{E},l} \sim \epsilon/l^2$, which diverges at $l \to 0$. The only solution is that while enstrophy is transferred from large to small scales, energy is transferred to scales larger than those of the forcing. This is indeed the situation observed in numerical simulations of 2D turbulence, with an enstrophy cascade to smaller scales and an energy cascade to larger scales simultaneously present

$$\tilde{u}_l \sim \begin{cases} (\epsilon/L^2)^{1/3} l, & l \ll L, \\ (\epsilon l)^{1/3}, & l \gg L. \end{cases} \tag{10.34}$$

The effect of helicity on the energy cascade in 3D flows is less dramatic. The fact that $\Pi_{I,l} \lesssim \Pi k, l/l = \epsilon/l$ allows to enforce simultaneously the condition that the two fluxes $\Pi_{k,l}$ and $\Pi_{I,l}$ are constant in scale: $\Pi_{I,l} = \epsilon_I \sim \epsilon/L$ and $\Pi_{k,l} = \epsilon$. It is not necessary to invoke energy and helicity cascades going in opposite directions. The Kolmogorov scaling in Eq. (10.13) at scales $k \ll L$ is the only one observed in experiments and numerical simulations.

10.2 Suggested reading

- P. Kundu, "Fluid Mechanics", Secs. 12.1-7 (Ac. Press 2015)